65153

JULY

1965

ROYAL AIRCRAFT ESTABLISHMENT

TECHNICAL REPORT No. 65153

THE EFFECT OF TRANSFER INJECTION ERRORS UPON THE ACCURACY OF HIGH CIRCULAR ORBITS

by

Keith Smith, B.Sc.(Eng). D.I.C.

MINISTRY OF AVIATION
FARNBOROUGH HANTS

U.D.C. No. 629.19.077.3 : 629.19.077.2

ROYAL AIRCRAFT ESTABLISHMENT

Technical Report No.65153

July 1965

THE EFFECT OF TRANSFER INJECTION ERRORS UPON THE ACCURACY OF HIGH CIRCULAR ORBITS

by

Keith Smith, B.Sc.(Eng) D.I.C.

SUMMARY

First-order relationships between the position and velocity errors at start and end of a Hohmann transfer are derived in a two-dimensional analysis. The results are then used to evaluate the effects of uncorrected first injection errors upon the mean radius and eccentricity of the final (nominally circular) orbit, assuming perfect application of the final impulsive velocity.

Finally the mean radius and eccentricity errors are expressed in terms of post-orbital velocities required for nulling, such as would be required in station-keeping communication satellite systems.

Departmental Reference: Space 102

CONTENTS

1 INTRODUCTION

When placing satellites into high circular orbits, the flight plan usually adopted consists of two phases of propelled motion (neglecting any specific requirements for parking). The first phase extends from launch to a condition in which propulsion ceases, resulting in the launch vehicle entering an elliptic orbit with a low perigee height and apogee close to the height of the final orbit. In practice the vehicle will enter the intermediate or "transfer" orbit close to perigee[3] and will coast until, just before apogee is reached, the second propulsive phase begins. This phase (of comparatively short duration compared with that of coasting transfer) continues until the vehicle has attained circular orbital speed at which time final injection is considered to have occurred.

High circular orbits are of prime interest in communication satellite systems, and in such cases it is often operationally difficult to monitor the parameters of the transfer ellipse, since this requires coverage by ground tracking stations. Consequently injection errors at the start of transfer (velocity and position) may remain uncorrected, resulting in final orbit errors additional to those incurred by imperfect propulsion during the second phase.

The object of this report is to determine the effect of errors at the start of transfer upon the errors in the major parameters of the final (nominally circular) orbit. The analysis is two-dimensional, and consequently the results are confined to in-plane errors. In order to simplify the analysis consideration is confined to the special case of Hohmann transfer. In this special case[1,2] coasting starts at perigee of the transfer ellipse and continues until apogee is reached, where application of a horizontal velocity impulse completes the injection.

The analysis contained in this report is divided into three logical phases.

(i) The derivation of first-order relationships between position and velocity errors at start of transfer to those at the end of transfer, using the well-established properties of ballistic trajectories[4,5]. In the first instance the relationships are expressed in a polar earth-centred axis system, but for the sake of completeness, these results are later transformed into a cartesian reference system. The latter system is likely to be the most suitable one in which to evaluate the error contributions of an inertial guidance system.

(ii) From the first phase it is possible to evaluate the consequent injection errors into the final orbit, assuming that the only errors are those at the start of transfer (i.e. the apogee impulse is applied as in the case of error-free transfer). Final injection errors are then transformed into the equivalent errors of the mean radius and eccentricity of the final (nominally circular) orbit.

(iii) Since many communication satellite systems involve accurate station-keeping for periods of years, it follows that such systems must be placed in orbits of exceedingly high accuracy. In order to achieve this accuracy in practice it will be necessary to make post-orbital velocity adjustments[7] by means of small thrust jet forces, located in the satellite itself. The velocity requirement from such a system will reflect in a direct loss of potential payload for communication purposes, and it is therefore useful to transform the orbit parameter errors of (ii) into equivalent velocity corrections. The corrections are defined as those necessary to null the mean radius and eccentricity errors of the final orbit.

2 BASIC ASSUMPTIONS OF THE ANALYSIS

2.1 Axis systems

As has already been mentioned, the present analysis is limited to two dimensions, and consequently does not cover the evaluation of the effects of errors normal to the plane of injection (which is also assumed to be the plane containing the final orbit). The primary analysis is undertaken in a polar axis system (see Fig.1) in which position is defined by two co-ordinates

r geocentric radius

and ϕ angular range

and velocity is defined by a further two

V magnitude of velocity vector

and θ direction of vector relative to the local horizontal (termed "climb angle")

2.2 The Hohmann transfer

The coasting transfer is considered to consist of an ellipse (termed "transfer ellipse"). The first phase of propulsion is assumed to terminate (in the error-free or nominal case) at the perigee of the ellipse, and the second phase begins at the apogee of the ellipse. Thus the vehicle coasts over exactly half of the ellipse. The second propulsive phase is taken as

consisting of an impulsive addition of velocity (locally horizontal in the error-free case), such that after the impulse has been applied the vehicle has achieved circular orbital velocity. At this point the vehicle is considered to be injected into the final orbit, and in the error-free case this orbit will be exactly circular. The transfer just described was first proposed by Hohmann[1]. The mathematical characteristics of such a transfer are well known[1,2] and are listed in Appendix A, and illustrated in Fig.2.

At first sight the assumption of using a Hohmann transfer in practice may seem to be rather sweeping. However, many practical launching systems will employ transfers which are close approximations to this ideal (e.g. the ELDO system described in Ref.3). Firstly, for optimum performance with real (finite thrust) vehicles it transpires that entry into the transfer ellipse occurs very close to perigee, especially if no altitude restrictions are placed on the first injection point from the point of view of obtaining satisfactory radio tracking coverage. Secondly, the finite acceleration encountered during the second propulsive phase is likely to be sufficiently high to approximate this phase to an impulse, especially if a spin-stabilised solid-propellant stage is used. Typically the angular range change during propulsion may be 5°, compared with 180° during the coasting transfer.

In view of these practical considerations, a Hohmann transfer is taken as the reference trajectory in the analysis of this report. The resulting simplification is considerable and the loss of accuracy in predicting the precise effect of injection errors negligible.

2.3 Magnitude of the errors

In the whole analysis of this report (see Appendices A, B and C) the relationships between input disturbances (i.e. position and velocity errors at start of transfer) and output quantities (i.e. errors at end of transfer or final orbit parameter errors or necessary corrective velocities) are linearised. Therefore the resulting equations can only be applied strictly if the perturbations are infinitely small, since second and higher order terms are neglected by implication. The approximation involved by such procedures is not likely to be serious however, since in practical launching systems the velocity injection errors at the start of transfer are likely to be of the order of tens of ft/sec compared with actual velocities of several thousands.

2.4 Application of impulsive velocity during the second burning phase

In the analysis it is assumed that the velocity impulse is added perfectly i.e. we are only investigating the effect of first injection errors upon the

final orbit. However, it is necessary to clarify what is meant by "perfect" application of the impulse. In the nominal case (i.e. no injection errors at the start of transfer) the impulse is applied at a time $T_o/2$ after start of transfer (where T_o is the orbital period of the nominal transfer ellipse) in a direction which is simultaneously parallel to the local horizontal and normal to the radius vector at the start of transfer (see Fig.2). The magnitude is $(V_{o_2} - V_2)$ where V_{o_2} is the circular orbital speed at the final radius r_2 and V_2 is the velocity at the end (apogee) of transfer (all values nominal). In the general perturbed case however, i.e. when first ejection errors are present, the local horizontal at the end of transfer (transfer being still considered to terminate after a time $T_o/2$ since no more tracking information is available) does not coincide with the direction nominal to the radius vector at nominal transfer start (e.g. see Fig.4), due to position errors at the end of transfer. We must therefore differentiate between two cases of "perfect" impulse application:- the first one in which the impulse is aligned parallel to the local horizontal at time $T_o/2$ after start of transfer, and the second one in which it is aligned in a space-fixed direction normal to the radius vector at nominal transfer start. Both methods of alignment are covered in this analysis since both can be achieved in practice. For example the first one is appropriate to alignment using sensors detecting the local horizontal (optical horizon sensors), and the second method would be realised using either inertial guidance or a spin stabilised final burning stage.

3 RESULTS OF THE ANALYSIS

3.1 Derivatives relating position and velocity errors at start of transfer to those at the end

3.1.1 Polar axis system

The detailed analysis is contained in Appendix A. The results enable the perturbations at beginning and end of transfer to be related in the form

$$|\delta y_2| = |M||\delta y_1| \qquad (1)$$

where $|\delta y_1|$ is the perturbation state vector at the start and $|\delta y_2|$ that at the end. Each of these vectors is four-dimensional, containing two position co-ordinates (r, ϕ) and two velocity co-ordinates (V, θ) as shown in Fig.2. The 4×4 matrix $|M|$ contains sixteen derivatives, all of which are evaluated in Appendix A and are tabulated, for the sake of completeness, in Table 1(a). The derivatives (other than those which are zero or unity) are plotted in

Figs.11, 12 and 13. The evaluation is in terms of a dimensionless parameter, termed "transfer ratio"

$$n = \frac{r_2}{r_1} \tag{2}$$

where r_1 is the radius at start of transfer

r_2 is the radius at end of transfer (also equal to the radius of the final circular orbit).

For generality to derivatives and normalised with respect to quantities which are dependent only upon the initial radius r_1, e.g. r_1 and V_{o_1} where

$$V_{o_1}^2 = \frac{\mu}{r_1} \tag{3}$$

V_{o_1} is the circular orbital speed at r_1

and μ is the earth's gravitational constant.

In Figs.11, 12 and 13 the derivatives are plotted non-dimensionally, but additional dimensional scales are provided for the special case in which the altitude at start of transfer is 300 nm. The numerical values taken in deriving the scaled derivatives are

Earth radius 3437.75 nautical miles

$$\mu = 1.40673 \times 10^{16} \text{ ft}^3/\text{sec}^2$$

$$1 \text{ nm} = 6080 \text{ ft} \quad .$$

3.1.2 Cartesian axis system

The results obtained in Appendix A have been transformed into an cartesian axis system, as shown in Fig.2. The detailed analysis of the transformation is contained in Appendix B and the results summarised in Table 1(b). The geometrical relationships between small perturbations in polar and cartesian axis are illustrated in Fig.8.

3.2 Derivatives relating position and velocity errors at start of transfer to mean radius and eccentricity errors of final orbit

In Appendix C, errors at the end of transfer are related to injection errors for the final orbit (assuming the two cases of "perfect" impulse previously described) and hence to errors in mean radius and eccentricity.

The results are shown (both dimensionally and non-dimensionally) in Figs.14, 15, 17, 19 and 20. Since, as is shown in Appendix C, eccentricity is a non-linear function of injection errors, we cannot apply the usual formula

$$\delta e = \left(\frac{\partial e}{\partial V_1}\right) \delta V_1 + \left(\frac{\partial e}{\partial \theta_1}\right) \delta\theta_1 + \left(\frac{\partial e}{\partial r_1}\right) \delta r_1 + \left(\frac{\partial e}{\partial \phi_1}\right) \delta\phi_1 \quad . \tag{4}$$

In the presence of a single input error it can be shown that a linear relationship will exist between input error and resulting eccentricity, provided the input error is replaced by its modulus, since positive eccentricity is produced by either positive or negative inputs, i.e.

$$\delta e \doteq \left(\frac{\partial e}{\partial V_1}\right) |\delta V_1| \text{ etc.} \tag{5}$$

where $(\partial e/\partial V_1)$ is positive.

In the presence of multiple input errors, equation (4) must be replaced by a more complex expression which will not be pursued here.

3.3 Derivatives relating position and velocity errors at start of transfer to post-orbital velocity corrections required to null orbital errors

In Appendix C the relations between post-orbital corrective velocity requirements and orbital errors are established, thereby making it possible to derive expressions for the corrective velocities in terms of errors at the start of transfer. Two velocity corrections are calculated, δu_a that necessary to null mean radius error, and δu_e, that for correcting eccentricity. Furthermore it is shown that both radius and eccentricity errors can be eliminated by a total impulse application equal to either δu_a or δu_e, which ever is the larger numerical quantity.

Once again, since δu_e is a non-linear function of δV_1, $\delta\theta_1$, δr_1 and $\delta\phi_1$ (even for small perturbations) it cannot be evaluated from a linear relation of the form of equation (4) when multiple inputs are present at the start of transfer.

Corrective velocity derivatives are plotted in Figs.16, 18 and 23. In Fig.18, $\partial u_e/\partial\theta_1$ is normalised by dividing by V_1 (rather than V_{o_1}) since $V_1\delta\theta_1$ is directly vertical velocity error. Hence Figs.16 and 18 now form a direct comparison of the relative effects of vertical and horizontal cut-off velocity errors. Similarly, in Fig.23 the scaled quantity plotted in the ordinate is $(\partial u_e/r_1\partial\phi_1)$. Now $r_1\delta\phi_1$ is the longitudinal position error, so that again we

can compare the relative effects of position errors in two directions from Figs.21 and 23.

4 DISCUSSION

4.1 Relations between errors at beginning and end of transfer

There is little comment that can be passed upon these results, except to mention their possible use in the overall detailed evaluation of any launcher guidance system that contains a Hohmann transfer (or a close approximation) in the flight plan. It was for this type of evaluation that the derivatives in Appendix A were converted into a cartesian axis system. Such a system of axes is the obvious choice for detailed investigation of inertial guidance errors, since most inertial navigators for space launchers will measure and navigate in these axes (e.g. Section 8 of Ref.7).

It is worth noting that initial errors in $\delta\theta_1$ and $\delta\phi_1$ perturb the transfer ellipse in a different way to errors in δV_1 and δr_1. The former produce no first order change in the mean radius of that orbit (resulting in zero change of radius or velocity at the end of transfer) while the latter produce changes in most of the transfer parameters (resulting in changes to all the co-ordinates at the end of transfer).

4.2 Errors in parameters of the final orbit

Errors in mean radius (δa) are only produced by δV_1 and δr_1 inputs (Figs.14 and 19), and these errors are independent of the method of aligning the apogee impulse (this only affects vertical velocity errors at injection). The mean height error for a given initial velocity error increases with transfer ratio, as does mean height error for a given initial radius error. Typical values for injection into a geo-stationary orbit (19450 nm altitude), assuming transfer to start at 300 nm altitude are

$$\frac{\partial a}{\partial V_1} = 10 \text{ nm/ft/sec}$$

and

$$\frac{\partial a}{\partial r_1} = 53 \text{ nm/nm} \quad .$$

Eccentricity δe results from any type of initial perturbation (Figs.15, 17, 20 and 22). For δV_1 and δr_1, δe, for a given initial disturbance, increases with transfer ratio. Also eccentricity can be minimised by aligning the apogee impulse to a fixed space direction rather than to the local horizontal, since in the former case the vertical velocity error at the end of transfer is partially

compensated by a locally opposite application of velocity during the impulse (i.e. $\partial\theta_2/\partial V_1$ is of opposite sign to $\partial\phi_2/\partial V_1$ and $\partial\theta_2/\partial r_1$ is of opposite sign to $\partial\phi_2/\partial r_1$). The effect of $\delta\theta_1$ or $\delta\phi_1$ errors is considerably different from that of δV_1 or δr_1. Firstly, the increasing effect with increasing transfer ratio is much less marked ($[\partial e/\partial\theta_1]_{k=o}$ actually decreases with increasing n,*) and secondly, the minimum eccentricity error is produced by aligning the apogee impulse to the local horizontal, rather than to a fixed space direction (actually $(\partial e/\partial\phi_1)_{k=o}$ is zero for all value of n).

For the geo-stationary orbit eccentricity derivatives are

$\left(\frac{\partial e}{\partial V_1}\right)_{k=o}$ = 0.00056 per ft/sec

$\left(\frac{\partial e}{\partial V_1}\right)_{k=1}$ = 0.00037 per ft/sec

$\left(\frac{\partial e}{\partial r_1}\right)_{k=o}$ = 0.00285 per nm

$\left(\frac{\partial e}{\partial r_1}\right)_{k=1}$ = 0.0018 per nm

$\left(\frac{\partial e}{\partial \theta_1}\right)_{k=o}$ = 0.09 per radian (or 0.0000027 per ft/sec of vertical velocity error)

$\left(\frac{\partial e}{\partial \theta_1}\right)_{k=1}$ = 1.17 per radian (or 0.000036 per ft/sec of vertical velocity error)

$\left(\frac{\partial e}{\partial \phi_1}\right)_{k=o}$ = 0 (or zero per nm of range error)

$\left(\frac{\partial e}{\partial \phi_1}\right)_{k=1}$ = 0.46 per radian (or 0.00012 per nm of range error)

We can see from these figures that horizontal velocity error (δV_1) has a larger effect upon final orbit eccentricity than vertical velocity error ($V_1\delta\theta_1$) even for k=1 (apogee impulse aligned in space), which is the case most favourable to δV_1 and least favourable to $\delta\theta_1$.

---

*The suffix k=o refers to the system with the apogee impulse aligned to the local horizontal, while k=1 corresponds to space alignment (see Appendix C, para. A3.2).

Similarly radial position error (δr_1) has a larger effect than range position error ($r_1 \delta\phi_1$).

4.3 Post-orbital corrective velocities

Before discussing the numerical values (Figs.16, 18, 21 and 23) it is appropriate to review the possible implications of corrective velocities upon a practical communication satellite launching system.

Firstly it must be noted that orbital period must be corrected to a very high degree of accuracy, since relative station keeping between individual satellites in the complete system must be maintained to within a few degrees over a period of several years. Since orbital period is directly related to mean radius (e.g. Ref.5), this implies that any initial mean radius error (δa) must be subsequently corrected to an extremely high degree of accuracy. In fact the final accuracy must be of the order of a fraction of an inch per second (in terms of velocity error) so that δu_a is, in practice, a good measure of the contribution that can be expected from first injection errors (other contributions can be expected from errors in the impulse itself, but these are not the subject of the present investigation). It must be remembered that δu_a is calculated here on the basis of tangential impulse, so that it is essential that practical post-orbital corrections should be capable of representation by such impulses.

Regarding correction of initial eccentricity error (δe) the situation is by no means so well defined. Residual eccentricity errors result only in cyclic station keeping errors (an eccentricity δe produces a sinusoidal phase error of amplitude $\pm 2\delta e$ and period equal to that of the nominal orbit). Some degree of cyclic error may be permissible in an actual communication system, although this will depend upon such details as the permissible movement of the ground aerials. Therefore the values of δu_e given here represent an upper limit to the corrective velocity that would be required.

Turning now to the present results, let us examine δu_a and δu_e required from an initial error δV_1 (Fig.16). Generally speaking both $\partial u_a/\partial V_1$ and $\partial u_e/\partial V_1$ increase with increasing transfer ratio, but with some slight variation to this rule for n between 1 and 2. For a synchronous orbit δu_a is larger than δu_e when the apogee impulse is aligned in space, while the reverse is true if the impulse is aligned to the local horizontal. As is explained in Appendix C, $\delta u_a > \delta u_e$ implies that the perturbed final orbit does not intercept the desired nominal circular orbit, while $\delta u_a < \delta u_e$ implies that interception does occur. Furthermore, if $\delta u_a > \delta u_e$ it means that eccentricity error can be nulled during the

mandatary process of orbital period correction. Also the positive margin between δu_a and δu_e allows some additional vertical velocity error to occur (e.g. from mis-direction of the apogee impulse) and still permit eccentricity nulling within the capability of δu_a.

From Fig.16, $\partial u_a/\partial V_1 = 2.2$ in a synchronous orbit. This emphasizes the importance of keeping uncorrected first injection forward velocity errors as small as possible, since their effect is magnified in relation to post-injection velocity requirements.

For an initial vertical velocity error $(V_1 \delta\theta_1)$ (see Fig.18), no correction is necessary for mean radius ($\delta u_a = 0$), and the correction for eccentricity is quite small ($1/V_1 \; \partial u_e/\partial\theta_1 = 0.18$ in the most unfavourable impulse alignment case).

For an initial radius error (δr_1) (see Fig.21), the corrective velocities are similar in form to those for δV_1. In a synchronous orbit

$$\frac{\partial u_a}{\partial r_1} = 11.5 \text{ ft/sec per nm}$$

and the eccentricity correction is slightly larger for the case of horizontal impulse alignment, and smaller for space alignment.

For a range error $(r_1 \delta\phi_1)$ there is no period correction required, and no eccentricity correction in the case of horizontal impulse alignment. For the case of space alignment $\partial u_e/r_1 \partial\phi_1 = 0.62$ ft/sec per nm (synchronous orbit) indicating that the effect of range errors is considerably smaller than that of height error.

4.4 Orbital errors and corrective velocities in the presence of multiple input errors

In any practical launching system errors will exist in all four co-ordinates at the first injection point (in addition to errors of the apogee impulse). Usually these individual errors will be defined statistically and it is desired to evaluate the effect of such errors upon final orbit parameters and corrective velocities. Such effects will again be derived in statistical form. Often it is possible to suppose that the "input" quantities are normally distributed, and uncorrelated with one another. If the "input"/"output" relationships are linear it is easy to show that the "output" quantities are also normally distributed and the standard deviation of the "output" is readily obtained in terms of the "input" standard deviation and the appropriate linear relationship. If the relationship is non-linear the statistical evaluation of "output" is more complex and no

general solution exists. Unfortunately, such is the case in the case of our "outputs", eccentricity (δe) and corrective velocity (δu_e). This problem has already been encountered in Ref.7. No solution is suggested here, the sole object of mentioning it being to advise exercise of caution in applying the results of this report.

5 CONCLUSIONS

(1) Derivatives have been evaluated, relating errors (position and velocity) at the start of a Hohmann transfer to those at the end. Such derivatives are of use in the detailed investigation of the accuracy of any guidance system employed in injecting satellites into high circular orbits (such as those required for communication satellite systems).

(2) These derivatives have been used to determine the effect of single errors at first injection upon the parameters of the final orbit, and the resulting necessary post injection corrective velocities. For large values of transfer ratio (final orbit radius divided by first injection radius) it has been shown that horizontal velocity errors are considerably more significant than vertical ones, while radial position errors have a larger effect than range position errors. As an example, for injection into a geo-stationary orbit each unit of horizontal velocity error will require at least 2.2 units of post orbital correction and each nautical mile of radial position error needs 11.5 ft/sec correction after injection.

Appendix A

PROPERTIES OF THE HOHMANN TRANSFER, INCLUDING RELATIONS BETWEEN SMALL PERTURBATIONS AT THE BEGINNING AND END OF THE TRANSFER PHASE, DERIVED IN A POLAR AXIS SYSTEM

A.1 General properties of the Hohmann transfer orbit

The ideal transfer (described in Refs.1, 2) consists of ballistic flight, extending over half of an ellipse, commencing at perigee and ending at apogee (Fig.2). The initial and final velocities of the transfer are defined in terms of the earth's gravitational constant (μ) and the initial and final geocentric radii (r_1 and r_2). The appropriate relations are

$$V_1 = V_{o_1} \sqrt{p_1} = V_{o_1} \sqrt{\frac{2n}{n+1}} \qquad (A.1)$$

$$V_2 = V_{o_2} \sqrt{p_2} = V_{o_2} \sqrt{\frac{2}{n+1}} \qquad (A.2)$$

where $V_{o_1} = \sqrt{\mu/r_1}$ is the circular orbital speed at the initial radius r_1

and $V_{o_2} = \sqrt{\mu/r_2}$ is the circular orbital speed at the final radius r_2.

The parameter p has been previously used in Ref.4 and is defined as the square of the ratio of speed to the circular orbital speed at the appropriate radius.

It will be noted that

$$\frac{V_1}{V_2} = \frac{V_{o_1}^2}{V_{o_2}^2} = n$$

where $n = r_2/r_1$.

The dimensionless parameter n (ratio of final to initial radii) will be termed the transfer ratio, and all derivatives relating initial and final perturbations will be expressed as a function of this quantity.

The transfer time is given by $T_o/2$, T_o being the orbital period of the transfer ellipse. Now orbital period is related simply to the mean radius of the orbit[5]:-

$$T_o = 2\pi \sqrt{\frac{a^3}{\mu}} \qquad (A.3)$$

where

$$a = \tfrac{1}{2}(r_1 + r_2) \; . \qquad (A.4)$$

The establishment of a circular orbit at radius r_2 is effected by adding a locally horizontal velocity impulse (of magnitude $V_{o_2} - V_2$) on arrival at the end of the transfer.

A.2 The effect of a small velocity perturbation δV_1 at the start of transfer

Consider the situation presented in Fig.4. Point S represents the start of the transfer and point E is the end point of the nominal (i.e. unperturbed) transfer. Now point A represents the apogee of the perturbed transfer ellipse. As illustrated, A is shown for a positive perturbation in V_1. Since A will occur later in time than E, the actual perturbed transfer will end at point E', assuming the impulsive velocity $(V_{o_2} - V_2)$ is added at the instant corresponding to the end of the nominal transfer.

A.2.1 V and r perturbation at end of transfer

Let δt be the perturbation in the half-period of the transfer ellipse, due to initial perturbation δV_1. Since $\dot{r} = 0$ at point A, the difference of radius vector between A and E' is of order $\ddot{r}(\delta t)^2$, where $\ddot{r}$ is described near to apogee. Since δt will be proportional to δV_1 (for small δV_1), we can neglect the difference between radius vectors at A and E' when evaluating derivatives describing the first order relationship between δV_1 and radius perturbation at E'. Similarly, since radii changes between A and E' are of 2nd order, compared with radii changes between E and A, we may also conclude that to a first order the velocity magnitude perturbation at E' (δV_2) equals that at A. This follows from the conservation of total energy[6] (kinetic plus potential) between A and E'.

We may therefore conclude that the velocity and radius perturbations at E' are equal to those at A, provided that δV_1 is small. Let us assume that the perturbations at A or E' are δV_2, δr_2 respectively. Then from the conservation of angular momentum between perigee and apogee[6], we have

$$V_1 r_1 = V_2 r_2 \quad \text{(nominal case)}$$

$$(V_1 + \delta V_1)\, r_1 = (V_2 + \delta V_2)\,(r_2 + \delta r_2) \quad \text{(perturbed case)} \ .$$

By differencing these equations:-

$$r_1 \delta V_1 = r_2 \delta V_2 + V_2 \delta r_2 \ . \qquad \text{(A.5)}$$

Note that again we have neglected the second order term $\delta V_2\, \delta r_2$.

Similarly from the conservation of total energy between apogee and perigee,

$$\tfrac{1}{2} V_1^2 - \frac{\mu}{r_1} = \tfrac{1}{2} V_2^2 - \frac{\mu}{r_2} \quad \text{(nominal case)}$$

$$\tfrac{1}{2}(V_1 + \delta V_1)^2 - \frac{\mu}{r_1} = \tfrac{1}{2}(V_2 + \delta V_2)^2 - \frac{\mu}{(r_2 + \delta r_2)} \quad \text{(perturbed case)} \ .$$

Again, by differencing and neglecting 2nd order terms

$$V_1 \delta V_1 = V_2 \delta V_2 + \frac{\mu}{r_2^2} \delta r_2 \ . \tag{A.6}$$

By solving equations (5) and (6) simultaneously,

$$\delta V_2 = \delta V_1 \frac{\left(r_1 - \frac{V_2 V_1 r_2^2}{\mu}\right)}{\left(r_2 - \frac{V_2^2 r_2^2}{\mu}\right)} \tag{A.7}$$

and

$$\delta r_2 = \delta V_1 \frac{\left(\frac{V_1 r_2^2}{\mu} - \frac{V_2 r_1 r_2}{\mu}\right)}{\left(1 - \frac{V_2^2 r_2}{\mu}\right)} \ . \tag{A.8}$$

The derivatives resulting from these two equations can be written in a more convenient, and non-dimensional form, using the formula for start and end velocities as given in equations (1) and (2):-

$$\boxed{\frac{\partial V_2}{\partial V_1} = -\left(2 + \frac{1}{n}\right)} \tag{A.9}$$

$$\boxed{\frac{V_{o_1}}{r_1} \cdot \frac{\partial r_2}{\partial V_1} = \sqrt{2n(1+n)^3}} \ . \tag{A.10}$$

A.2.2 θ and φ perturbation at the end of transfer

We have already seen that the apogee of the perturbed transfer ellipse is attained at a later time than the end of the nominal transfer (for positive δV_1).

This is because the mean height of the perturbed transfer ellipse is higher than that of the nominal one. If the perturbed apogee occurs δt later than that for the nominal, then $\delta t = \frac{1}{2}\delta T_o$, where δT_o is the increase in orbital period of the perturbed ellipse. Using equations (3) and (4) it is possible to relate δt to δr_2 and hence to δV_1 (for small perturbations). The result is

$$\delta t = \delta V_1 \cdot \frac{3\pi}{4}\sqrt{n}\,(1+n)^2 \cdot \frac{r_1^2}{\mu} \quad . \tag{A.11}$$

Now one of the equations of motion describing ballistic flight is

$$\dot{V\theta} = -\frac{\mu}{r^2}\cos\theta + \frac{V^2}{r}\cos\theta \quad .$$

Also $\theta = 0$ at point A, so that at E'

$$\delta\theta_2 = \left(\frac{\mu}{r_2^2} - \frac{V_2^2}{r_2}\right)\frac{\delta t}{V_2} \quad . \tag{A.12}$$

Combining equations (11) and (12) we obtain the following non-dimensional derivative relating terminal climb angle error to initial velocity error:-

$$\boxed{V_{o_1}\frac{\partial\theta_2}{\partial V_1} = \frac{3\pi}{4\sqrt{2}}(1+n)^{3/2}\left(1-\frac{1}{n}\right)} \quad . \tag{A.13}$$

To obtain $\delta\phi_2$ at the end of the perturbed transfer, we multiply $-\dot{\phi}_2$ by δt (the negative sign indicating that $\delta\phi_2$ is negative for positive δV_1). Again we obtain a normalised derivative (using $\dot{\phi}_2 = V_2/r_2$):-

$$\boxed{V_{o_1}\frac{\partial\phi_2}{\partial V_1} = -\frac{3\pi}{4n}\sqrt{2(1+n)^3}} \quad . \tag{A.14}$$

The derivatives given by equations (9), (10), (13) and (14) are plotted in Fig.11.

A.3 The effect of a small climb path perturbation at the start of transfer

This situation is presented in Fig.5. Point S represents the start of nominal and perturbed transfers. E is the end of the nominal transfer and P is the perigee of the perturbed transfer. For a positive $\delta\theta_1$ perturbation, P will occur before the start of transfer (as illustrated in Fig.5). Let P occur at a time $-\delta t$ (i.e. δt before start, where δt is not related to the δt used in para. A.2). Now from the equation of motion used previously, i.e.

$$\dot{V\theta} = -\frac{\mu}{r^2}\cos\theta + \frac{V^2}{r}\cos\theta$$

$\dot{\theta}$ near perigee equals $(V_1^2/r_1 - \mu/r_1^2)\ 1/V_1$, which is positive, so that

$$\delta t = \frac{\delta\theta_1}{\dot{\theta}} \quad \text{near perigee}$$

i.e.

$$\delta t = \frac{\delta\theta_1 V_1}{\left\{\frac{V_1^2}{r_1} - \frac{\mu}{r_1^2}\right\}} \quad . \qquad \text{(A.15)}$$

Now the radius r at perigee P is of the form

$$r_1 - K\delta t^2$$

i.e. of the form $r_1 - K'\delta\theta_1^2$, so that to a first order the perigee radius is unaltered from the nominal value r_1. Also the total energy of the perturbed transfer orbit is unaltered from that of the nominal one since the potential energy is unaltered and the velocity vector at S is only changed through a small angle $\delta\theta_1$. It also follows that the orbital period is unaltered as is the apogee radius (to a first order).

Let A be the apogee of the perturbed transfer (at radius r_2). This occurs at time $(T_o/2 - \delta t)$ after start of transfer. Point E' represents the end of perturbed transfer, where E' occurs δt after apogee A. (As previously, we are assuming that the perturbed transfer terminates at the same time instant as for the nominal transfer, i.e. $T_o/2$ after start.)

A.3.1 V and r perturbation at end of transfer

Since the total energy, perigee and apogee radii are identical for nominal and perturbed transfers, V and r at point A will be identical to the values at E.

Also, since E' occurs at a time δt after A, the radius at E' will differ from that A by a term proportional to δt^2, i.e. proportional to $\delta\theta_1^2$. Hence there is no r perturbation at E' compared with E, to a first order. Also, since there is no change in total energy due to perturbation there is no V perturbation at E' compared with E. We can simply write:-

$$\boxed{\frac{1}{V_{o_1}} \frac{\partial V_2}{\partial \theta_1} = 0} \qquad (A.16)$$

$$\boxed{\frac{1}{r_1} \frac{\partial r_2}{\partial \theta_1} = 0} \; . \qquad (A.17)$$

A.3.2 θ and ϕ perturbations at end of transfer

Near apogee, from the previously used equation of motion

$$\overset{o}{\theta} = -\frac{1}{V_2}\left(\frac{\mu}{r_2^2} - \frac{V_2^2}{r_2}\right)$$

so that at E', $\delta\theta_2$ equals $\overset{o}{\theta}\,\delta t$. From equation (A.15) this gives

$$\delta\theta_2 = \frac{-\frac{\delta\theta_1 V_1}{V_2}\left[\frac{\mu}{r_2^2} - \frac{V_2^2}{r_2}\right]}{\left[\frac{V_1^2}{r_1} - \frac{\mu}{r_1^2}\right]} \; .$$

Using the previously established relations between V_1, V_2, r_1 and r_2 this reduces to the dimensionless form:-

$$\boxed{\frac{\partial \theta_2}{\partial \theta_1} = -\frac{1}{n}} \; . \qquad (A.18)$$

Referring to Fig.5, the angular range perturbation at E' is $\delta\phi_2$, where $\delta\phi_2 = -\delta\alpha + \delta\beta$.

Now

$$\delta\alpha = \delta t \times \text{angular velocity near perigee} = \frac{\delta t\, V_1}{r_1}$$

and $$\delta\beta = \delta t \times \text{angular velocity near apogee} = \frac{\delta t\, V_2}{r_2} \quad .$$

So that

$$\delta\phi_2 = \delta t \left\{ \frac{V_2}{r_2} - \frac{V_1}{r_1} \right\} \quad . \qquad \text{(A.19)}$$

Substituting for δt from (A.15), we can obtain the dimensionless form

$$\boxed{\frac{\partial \phi_2}{\partial \theta_1} = -2\left(1 + \frac{1}{n}\right)} \quad . \qquad \text{(A.20)}$$

The derivatives $\partial\theta_2/\partial\theta_1$ and $\partial\phi_2/\partial\theta_1$ are plotted in Fig.12.

A.4 The effect of a small radial perturbation at the start of transfer

Fig.6 illustrates the geometry of the nominal and perturbed transfer; S is the nominal start point and S' the perturbed one. E represents the nominal transfer end and A the apogee of perturbed transfer ellipse. Since A occurs at time $(T_o/2 + \delta t)$, once again we have the perturbed end occurring at E', some distance before A.

As was shown in para. A.2, the V and r perturbations that exist at A are, to a first order, identical to those at E', since E' is close to apogee.

A.4.1 V and r perturbations at end of transfer

Let the perturbations at A (or E') be δV_2 in velocity and δr_2 in radius. Pursuing the same technique as was used in para. A.2.1 we have, from the conservation of angular momentum, and total energy

$$V_1 r_1 = V_2 r_2$$

$$V_1 (r_1 + \delta r_1) = (V_2 + \delta V_2)(r_2 + \delta r_2)$$

giving

$$V_1 \delta r_1 = r_2 \delta V_2 + V_2 \delta r_2 \qquad \text{(A.21)}$$

and also

$$\tfrac{1}{2} V_1^2 - \mu/r_1 = \tfrac{1}{2} V_2^2 - \mu/r_2$$

$$\tfrac{1}{2} V_1^2 - \mu/r_1 + \delta r_1 = \tfrac{1}{2} (V_2 + \delta V_2)^2 - \mu/(r_2 + \delta r_2)$$

giving

$$\mu/r_1^2 \, \delta r_1 = V_2 \, \delta V_2 + \mu/r_2^2 \, \delta r_2 \quad . \tag{A.22}$$

Solving equations (A.21) and (A.22) simultaneously we obtain the dimensionless derivatives:-

$$\boxed{\frac{r_1}{V_{o_1}} \cdot \frac{\partial V_2}{\partial r_1} = -\sqrt{2\left(1+\frac{1}{n}\right)}} \tag{A.23}$$

$$\boxed{\frac{\partial r_2}{\partial r_1} = n(n+2)} \; . \tag{A.24}$$

A.4.2 θ and φ perturbations at end of transfer

Since A occurs at time $T_o/2 + \delta t$, where $2\delta t = \delta T_o$, the perturbation in the orbital period of the transfer ellipse, we can obtain δt from equations (A.3), (A.4) and (A.24):-

$$\delta t = \delta r_1 \frac{3\pi}{4} \sqrt{\frac{r_1}{\mu} \frac{(1+n)^5}{2}} \quad . \tag{A.25}$$

But the perturbed end occurs at time $T_o/2$, so that at E'

$$\delta\theta_2 = -\overset{o}{\theta} \text{ near apogee} \times \delta t \; .$$

But

$$\overset{\varphi}{\theta} = \left(\frac{V_2^2}{r_2} - \frac{\mu}{r_2^2}\right) \frac{1}{V_2}$$

so that

$$\delta\theta_2 = \delta r_1 \frac{3\pi}{4} \sqrt{\frac{r_1}{\mu} \frac{(1+n)^5}{2}} \frac{1}{V_2} \left(\frac{\mu}{r_2^2} - \frac{V_2^2}{r_2}\right) \; .$$

This can be reduced to the non-dimensional form:-

$$r_1 \frac{\partial \theta_2}{\partial r_1} = \frac{3\pi}{8n} \frac{(n-1)(n+1)^2}{\sqrt{n}} \quad . \tag{A.26}$$

Also, the perturbed transfer end occurs at an angular range with perturbation

$$\delta\phi_2 = -\delta t \times \text{angular velocity near apogee} \quad .$$

But the angular velocity near apogee is V_2/r_2, so that

$$\delta\phi_2 = -\delta t \frac{V_2}{r_2} \quad . \tag{A.27}$$

Substituting (A.25) in (A.27), we obtain the non-dimensional derivative

$$r_1 \frac{\partial \phi_2}{\partial r_1} = -\frac{3\pi}{4} \frac{(1+n)^2}{n\sqrt{n}} \quad . \tag{A.28}$$

The derivatives from equations (A.23), (A.24), (A.26) and (A.28) are plotted in Fig.13.

A.5 The effect of a small angular range perturbation at the start of transfer

The effects of this initial perturbation are simple to visualise (see Fig.7). Since the apogee and perigee radii and the corresponding velocities are independent of the angular position at first injection it is reasonable to conclude that the only perturbation to the transfer ellipse is in respect of the orientation of the major axis. This resulting change in orientation equals the initial perturbation $\delta\phi_1$.

Thus, quite simply

$$\frac{1}{V_{o_1}} \frac{\partial V_2}{\partial \phi_1} = 0 \tag{A.29}$$

$$\frac{1}{r_1} \frac{\partial r_2}{\partial \phi_1} = 0 \tag{A.30}$$

$$\boxed{\frac{\partial \theta_2}{\partial \phi_1} = 0} \qquad \text{(A.31)}$$

$$\boxed{\frac{\partial \phi_2}{\partial \phi_1} = 1} \qquad \text{(A.32)}$$

Appendix B

DERIVATIVES RELATING PERTURBATIONS AT START OF TRANSFER TO THOSE AT THE END: CONVERSION FROM POLAR TO CARTESIAN AXES SYSTEMS

B.1 Definition of axes systems

The relevant systems are illustrated in Fig.1. In the polar system position is defined r (geocentric radius) and angular range ϕ (the datum of which is arbitrarily taken as the vertical at the point of commencing the nominal Hohmann transfer). Velocity is defined by magnitude V and climb path relative to local horizontal, θ.

In the cartesian system, position is defined by two co-ordinates x, and z. These axes are orthogonal and inertially fixed. The origin is at the earth centre O and Ox is parallel to the velocity vector at nominal transfer start. Consequently Oz is parallel to the ϕ datum in the polar system and is arbitrarily considered to be positive when vertically upwards at this point. The nominal start and end conditions for transfer, in the two systems are obvious, and are illustrated in Fig.2 for the polar case. In cartesian axes the conditions are given in Fig.3, and are as follows:-

Initial

$$x = x_1 = 0$$
$$z = z_1 = r_1$$
$$\dot{x} = \dot{x}_1 = V_1$$
$$\dot{z} = \dot{z}_1 = 0$$

Final

$$x = x_2 = 0$$
$$z = z_2 = -r_2$$
$$\dot{x} = \dot{x}_2 = -V_2$$
$$\dot{z} = \dot{z}_2 = 0$$

B.2 Relation between polar and cartesian perturbations

These are shown in Fig.8. At the start of transfer the relationships are (for small perturbations)

$$\delta r_1 = \delta z_1 \qquad \text{(B.1)}$$

$$\delta \phi_1 = \frac{1}{r_1} \delta x_1 \qquad \text{(B.2)}$$

$$\delta V_1 = \delta \overset{o}{x}_1 \tag{B.3}$$

$$\delta\theta = \frac{1}{V_1}\,\delta \overset{o}{z}_1 + \frac{1}{r_1}\,\delta x_1 \quad . \tag{B.4}$$

The above relations are derived from geometrical considerations together with the assumption that $\sin \delta\theta_1 \simeq \delta\theta_1$ and $\cos \delta\theta_1 \simeq 1$.

At the end of transfer the inverse expressions can be derived by similar considerations:-

$$\delta x_2 = -r_2\,\delta\phi_2 \tag{B.5}$$

$$\delta z_2 = -\delta r_2 \tag{B.6}$$

$$\delta \overset{o}{x}_2 = -\delta V_2 \tag{B.7}$$

$$\delta \overset{o}{z}_2 = -V_2\,\delta\theta_2 + V_2\,\delta\phi_2 \quad . \tag{B.8}$$

B.3 Basic expressions relating cartesian and polar derivatives

In polar co-ordinates, initial and final perturbations are related by the following expressions

$$\delta r_2 = \frac{\partial r_2}{\partial r_1}\,\delta r_1 + \frac{\partial r_2}{\partial \phi_1}\,\delta\phi_1 + \frac{\partial r_2}{\partial V_1}\,\delta V_1 + \frac{\partial r_2}{\partial \theta_1}\,\delta\theta_1 \tag{B.9}$$

$$\delta\phi_2 = \frac{\partial \phi_2}{\partial r_1}\,\delta r_1 + \frac{\partial \phi_2}{\partial \phi_1}\,\delta\phi_1 + \frac{\partial \phi_2}{\partial V_1}\,\delta V_1 + \frac{\partial \phi_2}{\partial \theta_1}\,\delta\theta_1 \tag{B.10}$$

$$\delta V_2 = \frac{\partial V_2}{\partial r_1}\,\delta r_1 + \frac{\partial V_2}{\partial \phi_1}\,\delta\phi_1 + \frac{\partial V_2}{\partial V_1}\,\delta V_1 + \frac{\partial V_2}{\partial \theta_1}\,\delta\theta_1 \tag{B.11}$$

$$\delta\theta_2 = \frac{\partial \theta_2}{\partial r_1}\,\delta r_1 + \frac{\partial \theta_2}{\partial \phi_1}\,\delta\phi_1 + \frac{\partial \theta_2}{\partial V_1}\,\delta V_1 + \frac{\partial \theta_2}{\partial \theta_1}\,\delta\theta_1 \quad . \tag{B.12}$$

Substituting in equations (B.9) to (B.12) for the expressions of δr_1, $\delta\phi_1$, δV_1, $\delta\theta_1$ and δr_2, $\delta\phi_2$, δV_2, $\delta\theta_2$ obtained in equations (B.1) to (B.8) we can now relate start and end perturbations in the cartesian axis system, i.e.

$$\delta x_2 = - r_2 \frac{\partial \phi_2}{\partial V_1} \delta \overset{\circ}{x}_1 - r_2 \frac{\partial \phi_2}{\partial r_1} \delta z_1 - r_2 \frac{\partial \phi_2}{\partial \theta_1} \left(\frac{1}{V_1} \delta \overset{\circ}{z}_1 + \frac{1}{r_1} \delta x_1 \right) - \frac{r_2}{r_1} \frac{\partial \phi_2}{\partial \phi_1} \delta x_1 \quad \ldots\ldots (B.13)$$

$$\delta z_2 = - \frac{\partial r_2}{\partial V_1} \delta \overset{\circ}{x}_1 - \frac{\partial r_2}{\partial r_1} \delta z_1 - \frac{\partial r_2}{\partial \theta_1} \left(\frac{1}{V_1} \delta \overset{\circ}{z}_1 + \frac{1}{r_1} \delta x_1 \right) - \frac{1}{r_1} \frac{\partial r_2}{\partial \phi_1} \delta x_1 \quad (B.14)$$

$$\delta \overset{\circ}{x}_2 = - \frac{\partial V_2}{\partial V_1} \delta \overset{\circ}{x}_1 - \frac{\partial V_2}{\partial r_1} \delta z_1 - \frac{\partial V_2}{\partial \theta_1} \left(\frac{1}{V_1} \delta \overset{\circ}{z}_1 + \frac{1}{r_1} \delta x_1 \right) - \frac{\partial V_2}{\partial \phi_1} \frac{1}{r_1} \delta x_1 \quad (B.15)$$

$$\delta \overset{\circ}{z}_2 = V_2 \left\{ \frac{\partial \phi_2}{\partial V_1} - \frac{\partial \phi_2}{\partial V_1} \right\} \delta \overset{\circ}{x}_1 + V_2 \left\{ \frac{\partial \phi_2}{\partial r_1} - \frac{\partial \theta_2}{\partial r_1} \right\} \delta z_1$$

$$+ V_2 \left\{ \frac{\partial \phi_2}{\partial \theta_1} - \frac{\partial \theta_2}{\partial \theta_1} \right\} \left\{ \frac{1}{V_1} \delta \overset{\circ}{z}_1 + \frac{1}{r_1} \delta x_1 \right\} + V_2 \left\{ \frac{\partial \phi_2}{\partial \phi_1} - \frac{\partial \theta_2}{\partial \phi_1} \right\} \frac{1}{r_1} \delta x_1 \quad . \quad (B.16)$$

But by definition

$$\delta x_2 = \frac{\partial x_2}{\partial x_1} \delta x_1 + \frac{\partial x_2}{\partial z_1} \delta z_1 + \frac{\partial x_2}{\partial \overset{\circ}{x}_1} \delta \overset{\circ}{x}_1 + \frac{\partial x_2}{\partial \overset{\circ}{z}_1} \delta \overset{\circ}{z}_1$$

$$\delta z_2 = \frac{\partial z_2}{\partial x_1} \delta x_1 + \frac{\partial z_2}{\partial z_1} \delta z_1 + \frac{\partial z_2}{\partial \overset{\circ}{x}_1} \delta \overset{\circ}{x}_1 + \frac{\partial z_2}{\partial \overset{\circ}{z}_1} \delta \overset{\circ}{z}_1$$

etc.

By equating terms we can first relate cartesian and polar derivatives in the following dimensional form:-

$$\frac{\partial x_2}{\partial x_1} = - \frac{r_2}{r_1} \left(\frac{\partial \phi_2}{\partial \theta_1} + \frac{\partial \phi_2}{\partial \phi_1} \right)$$

$$\frac{\partial x_2}{\partial z_1} = - r_2 \frac{\partial \phi_2}{\partial r_1}$$

$$\frac{\partial x_2}{\partial \overset{o}{x}_1} = - r_2 \frac{\partial \phi_2}{\partial V_1}$$

$$\frac{\partial x_2}{\partial \overset{o}{z}_1} = - \frac{r_2}{V_1} \frac{\partial \phi_2}{\partial \theta_1}$$

$$\frac{\partial z_2}{\partial x_1} = - \frac{1}{r_1} \left\{ \frac{\partial r_2}{\partial \theta_1} + \frac{\partial r_2}{\partial \phi_1} \right\}$$

$$\frac{\partial z_2}{\partial z_1} = - \frac{\partial r_2}{\partial r_1}$$

$$\frac{\partial z_2}{\partial \overset{o}{x}_1} = - \frac{\partial r_2}{\partial V_1}$$

$$\frac{\partial z_2}{\partial \overset{o}{z}_1} = - \frac{1}{V_1} \frac{\partial r_2}{\partial \theta_1}$$

$$\frac{\partial \overset{o}{x}_2}{\partial x_1} = - \frac{1}{r_1} \left\{ \frac{\partial V_2}{\partial \phi_1} + \frac{\partial V_2}{\partial \theta_1} \right\}$$

$$\frac{\partial \overset{o}{x}_2}{\partial z_1} = - \frac{\partial V_2}{\partial r_1}$$

$$\frac{\partial \overset{o}{x}_2}{\partial \overset{o}{x}_1} = - \frac{\partial V_2}{\partial V_1}$$

$$\frac{\partial \overset{o}{x}_2}{\partial \overset{o}{z}_1} = - \frac{1}{V_1} \frac{\partial V_2}{\partial \theta_1}$$

$$\frac{\partial \overset{o}{z}_2}{\partial x_1} = \frac{V_2}{r_1} \left\{ \frac{\partial \phi_2}{\partial \theta_1} - \frac{\partial \theta_2}{\partial \theta_1} \right\} + \frac{V_2}{r_1} \left\{ \frac{\partial \phi_2}{\partial \phi_1} - \frac{\partial \theta_2}{\partial \phi_1} \right\}$$

$$\frac{\partial z_2^o}{\partial z_1} = V_2 \left\{ \frac{\partial \phi_2}{\partial r_1} - \frac{\partial \theta_2}{\partial r_1} \right\}$$

$$\frac{\partial z_2^o}{\partial x_1^o} = V_2 \left\{ \frac{\partial \phi_2}{\partial V_1} - \frac{\partial \theta_2}{\partial V_1} \right\}$$

$$\frac{\partial z_2^o}{\partial z_1^o} = \frac{V_2}{V_1} \left\{ \frac{\partial \phi_2}{\partial \theta_1} - \frac{\partial \theta_2}{\partial \theta_1} \right\}$$

B.4 Normalised cartesian derivatives

These cartesian derivatives can be normalised, using the previously established normalised polar derivatives and the various relationships between V_1, V_2, r_1 and r_2 (see Appendix A). The results are as follows:-

$$\frac{\partial x_2}{\partial x_1} = n+2$$

$$\frac{\partial x_2}{\partial z_1} = \frac{3\pi}{4} \frac{(1+n)^2}{\sqrt{n}}$$

$$\frac{V_{o_1}}{r_1} \frac{\partial x_2}{\partial x_1^o} = \frac{3\pi}{4} \sqrt{2(1+n)^3}$$

$$\frac{V_{o_1}}{r_1} \frac{\partial x_2}{\partial z_1^o} = \sqrt{\frac{2(1+n)^3}{n}}$$

$$\frac{\partial z_2}{\partial x_1} = 0$$

$$\frac{\partial z_2}{\partial z_1} = -n\,(n+2)$$

$$\frac{V_{o_1}}{r_1}\frac{\partial z_2}{\partial x_1^o} = -\sqrt{2n(1+n)^3}$$

$$\frac{V_{o_1}}{r_1}\frac{\partial z_2}{\partial z_1^o} = 0$$

$$\frac{r_1}{V_{o_1}}\frac{\partial x_2^o}{\partial x_1} = 0$$

$$\frac{r_1}{V_{o_1}}\frac{\partial x_2^o}{\partial z_1} = \sqrt{2\left(1+\frac{1}{n}\right)}$$

$$\frac{\partial x_2^o}{\partial x_1^o} = \left(2+\frac{1}{n}\right)$$

$$\frac{\partial x_2^o}{\partial z_1^o} = 0$$

$$\frac{r_1}{V_{o_1}}\frac{\partial z_2^o}{\partial x_1} = -\sqrt{\frac{2(1+n)}{n^3}}$$

$$\frac{r_1}{V_{o_1}}\frac{\partial z_2^o}{\partial z_1} = -\frac{3\pi}{4\sqrt{2}\,n^2}(1+n)^{5/2}$$

$$\frac{\partial z_2^o}{\partial x_1^o} = -\frac{3\pi}{4n\sqrt{n}}(1+n)^2$$

$$\frac{\partial z_2^o}{\partial z_1^o} = -\frac{(1+2n)}{n^2} \quad .$$

Appendix C

DERIVATIVES RELATING ERRORS IN FINAL (NOMINALLY CIRCULAR) ORBIT TO ERRORS AT START OF HOHMANN TRANSFER - FINAL IMPULSE ASSUMED TO BE APPLIED WITHOUT ERROR

C.1 Errors in the orbital parameters of a nominally circular orbit, expressed in terms of injection errors

We shall consider only the effects upon two orbital parameters, namely mean radius and eccentricity.

General expressions for these parameters, in terms of cut-off conditions have been given in many forms, but equations in a convenient manner for our present purposes can be found in Refs.5, 6. They are:

Mean radius

$$a = \frac{r}{2-p} \tag{C.1}$$

Eccentricity

$$e = \sqrt{(1-p)^2 + p(2-p)\sin^2\theta} \tag{C.2}$$

where

$$p = \frac{rV^2}{\mu} \tag{C.3}$$

is a non-dimensional parameter already introduced in Appendix A. r, V and θ describe position and velocity at injection, in a polar axis system (see Fig.1).

For injection into a perfectly circular orbit $p = 1$ and $\theta = 0$. Let us now consider the effects of small errors in r, V and θ upon the resulting errors in a and e.

Let the small perturbations be δr, δV, $\delta\theta$ respectively. Then, from equation (C.3), and neglecting second order terms,

$$p = 1 + \frac{\delta r}{r} + \frac{2\delta V}{V_o} \tag{C.4}$$

where $V_o = \sqrt{\mu/r}$ is circular orbital speed at radius r.

Substituting in equation (C.1) we get

$$a + \delta a = r + \delta a = \frac{r + \delta r}{1 - \frac{\delta r}{r} \frac{2\delta V}{V_o}} .$$

Hence

$$\boxed{\delta a = 2\delta r + \frac{2\delta V r}{V_o}} \qquad (C.5)$$

$$\boxed{\delta e = \sqrt{\left(\frac{\delta r}{r} + \frac{2\delta V}{V_o}\right)^2 + \delta\theta^2}} . \qquad (C.6)$$

It will be noted that δa is independent of $\delta\theta$. This is to be expected since a is a direct measure of the total energy of the orbit, which depends upon V and r, but not upon θ, the direction of the velocity vector.

In equation (C.3), the positive sign is taken outside the square root. This is because injection perturbations can only produce positive eccentricity; negative eccentricity has no physical significance.

C.2 Relation between perturbations at end of Hohmann transfer and those at injection into final orbit

We have already seen, in Appendix A, that the conditions at the end of the Hohmann transfer are as follows:-

Quantity	Nominal value	Perturbation
V	V_2	δV_2
θ	0	$\delta\theta_2$
r	r_2	δr_2
ϕ	π	$\delta\phi_2$

Following the application of an impulsive velocity at the end of transfer the position parameters (r, ϕ) will not change, but those describing velocity (V, θ) will, and the resulting velocity vector must be defined before we can formulate the injection errors into the final (nominally circular) orbit. The vector addition of velocities at the end of transfer is described in Fig.9. Vector 1 represents the velocity at end of transfer ($V = V_2 + \delta V_2$, $\theta = \delta\theta_2$). Vector 2 represents the impulse added, and since this is assumed to be perfect (i.e. the same as that required for nominal transfer) its magnitude is $(V_{o_2} - V_2)$.

However, its direction can be defined in two ways, both of which are correct for the nominal transfer case. The first way is to define the direction of impulse relative to the local horizontal at the end of transfer. Obviously the impulse $(V_{o_2} - V_2)$ should be applied parallel to the local horizontal and we shall assume that in the perturbed transfer it is still applied parallel to the local horizontal (such would be the case if, in practice, the apogee rocket were aligned by means of horizon sensors). The second way is to define the direction of the impulse as fixed in space, and to assume that this inertial direction is maintained even in the perturbed transfer condition. (This would correspond to the practical case in which an inertial reference, such as a gyro or spin stabilisation was used to align the apogee rocket.) Clearly the space-fixed direction along which the impulse $(V_{o_2} - V_2)$ would act is parallel to the local horizontal at the end of nominal transfer, but in general this inertial direction does not coincide with the local horizontal in the perturbed transfer condition.

Referring to Fig.9 we see that the velocity vector after adding the impulse (vector 3, which is the sum of vectors 1 and 2) has the following properties:-

Magnitude

$$(V_2 + \delta V_2) + (V_{o_2} - V_2) = V_{o_2} + \delta V_2$$

(assuming $\delta\theta_2$, $\delta\phi_2$ are small so that $\cos \delta\theta_2$, $\cos \delta\phi_2 = 1$).

Vertical component (relative to local horizontal)

$$(V_2 + \delta V_2)\, \delta\theta_2 + K(V_{o_2} - V_2)\, \delta\phi_2$$

where K = 0 corresponds to the case in which the impulse is aligned along the local horizontal

and K = 1 corresponds to the case in which the impulse is aligned in a space-fixed direction.

The resulting climb angle $\delta\theta_2'$ is given by

$$\delta\theta_2' = \frac{\text{vertical velocity component}}{V_{o_2}}$$

i.e.

$$\delta\theta_2' = \frac{V_2}{V_{o_2}}\delta\theta_2 + K\left(\frac{V_{o_2}-V_2}{V_{o_2}}\right)\delta\phi_2 = \sqrt{p_2}\,\delta\theta_2 + K\,(1-\sqrt{p_2})\,\delta\phi_2$$

(neglecting second order terms).

We can now tabulate all four perturbations at injection into the final orbit:-

Quantity	Nominal value	Perturbation
V	V_{o_2}	δV_2
θ	0	$\delta\theta_2' = \sqrt{p_2}\,\delta\theta_2 + K(1-\sqrt{p_2})\,\delta\phi_2$
r	r_2	δr_2
ϕ	π	$\delta\phi_2$

C.3 Relations between errors at start of transfer and errors in final orbit parameters

C.3.1 Mean radius

Using equation (C.5) and the tabulation of perturbations at injection into the final orbit we can derive the mean radius error of the final orbit, i.e.

$$\delta a = 2\delta r_2 + \frac{2r_2}{V_{o_2}}\delta V_2 \quad . \qquad (C.7)$$

Consider as an example, the effect of a perturbation δV_1 at the start of transfer. Then

$$\delta r_2 = \frac{\partial r_2}{\partial V_1}\delta V_1$$

$$\delta V_2 = \frac{\partial V_2}{\partial V_1}\delta V_1$$

where the derivatives $\partial r_2/\partial V_1$, $\partial V_2/\partial V_1$ have been derived in Appendix A.

Substituting these expressions in equation (C.7) we get:

$$\delta a = \frac{\partial a}{\partial V_1}\,\delta V_1 = \left(2\,\frac{\partial r_2}{\partial V_1} + \frac{2r_2}{V_{o_2}}\,\frac{\partial V_2}{\partial V_1}\right)\delta V_1$$

so that

$$\frac{\partial a}{\partial V_1} = 2\,\frac{\partial r_2}{\partial V_1} + \frac{2r_2}{V_{o_2}}\,\frac{\partial V_2}{\partial V_1} \quad . \tag{C.8}$$

This relationship between derivatives can be expressed in a more convenient non-dimensional form

i.e.
$$\boxed{\frac{V_{o_1}}{r_1}\,\frac{\partial a}{\partial V_1} = 2\left(\left[\frac{V_{o_1}}{r_1}\,\frac{\partial r_2}{\partial V_1}\right] + n\sqrt{n}\left(\frac{\partial V_2}{\partial V_1}\right)\right]} \quad . \tag{C.9}$$

This expression is derived by remembering that

$$\frac{r_2}{r_1} = \frac{V_{o_1}^2}{V_{o_2}^2} = n \quad \text{(see Appendix A)} \quad .$$

Similar expressions relating mean radius error to other perturbations at the start of transfer can also be derived by a similar process. The results are as follows:

$$\boxed{\frac{1}{r_1}\,\frac{\partial a}{\partial \theta_1} = 2\left[\left(\frac{1}{r_1}\,\frac{\partial r_2}{\partial \theta_1}\right) + n\sqrt{n}\left(\frac{1}{V_{o_1}}\,\frac{\partial V_2}{\partial \theta_1}\right)\right]} \tag{C.10}$$

$$\boxed{\frac{\partial a}{\partial r_1} = 2\left[\left(\frac{\partial r_2}{\partial r_1}\right) + n\sqrt{n}\left(\frac{r_1}{V_{o_1}}\,\frac{\partial V_2}{\partial r_1}\right)\right]} \tag{C.11}$$

$$\boxed{\frac{1}{r_1}\,\frac{\partial a}{\partial \phi_1} = 2\left[\left(\frac{1}{r_1}\,\frac{\partial r_2}{\partial \phi_1}\right) + n\sqrt{n}\left(\frac{1}{V_{o_1}}\,\frac{\partial V_2}{\partial \phi_1}\right)\right]} \quad . \tag{C.12}$$

Two points are of immediate interest. Firstly, mean radius error is, to a first order, independent of K (the method of aligning the impulse) since the direction of this impulse only effects vertical velocity at final injection. Secondly

$$\left(\frac{1}{r_1}\ \frac{\partial a}{\partial \theta_1}\right) = \left(\frac{1}{r}\ \frac{\partial a}{\partial \phi_1}\right) = 0 \quad \text{for all values of n}$$

since in Appendix A it was shown that $\partial r_2/\partial\theta_1$, $\partial V_2/\partial\theta_1$, $\partial r_2/\partial\phi_1$, and $\partial V_2/\partial\phi_1$ are all zero.

The results of equations (C.9) and (C.11) are plotted in Figs.14 and 19 respectively.

C.3.2 Eccentricity

Using equation (C.6) and the tabulation of perturbations at injection into the final orbit we have the eccentricity of the final orbit, i.e.

$$\delta e = \sqrt{\left(\frac{\delta r_2}{r_2} + \frac{2\delta V_2}{V_2}\right)^2 + \left(\sqrt{p_2}\ \delta\theta_2 + K\ [1-\sqrt{p_2}]\ \delta\phi_2\right)^2} \quad . \qquad (C.13)$$

Consider now the effect of a perturbation δV_1:-

we have

$$\delta r_2 = \frac{\partial r_2}{\partial V_1}\,\delta V_1$$

$$\delta V_2 = \frac{\partial V_2}{\partial V_1}\,\delta V_1$$

$$\delta\theta_2 = \frac{\partial \theta_2}{\partial V_1}\,\delta V_1$$

and

$$\delta\phi_2 = \frac{\partial \phi_2}{\partial V_1}\,\delta V_1 \quad .$$

Giving

$$\delta e = \pm\delta V_1 \sqrt{\left(\frac{1}{r_2}\ \frac{\partial r_2}{\partial V_1} + \frac{2}{V_2}\ \frac{\partial V_2}{\partial V_1}\right)^2 + \left(\sqrt{p_2}\ \frac{\partial \theta_2}{\partial V_1} + K\ [1-\sqrt{p_2}]\ \frac{\partial \phi_2}{\partial V_1}\right)^2} \quad . \qquad (C.14)$$

The sign on the right hand side of equation (C.14) needs some explanation. Clearly, since negative eccentricities cannot exist, the positive sign must apply if δV_1 is positive and the negative sign is used if δV_1 is negative.

We can therefore define $\partial e/\partial V_1$ as

$$+\sqrt{\left(\frac{1}{r_2}\ \frac{\partial r_2}{\partial V_1}+\frac{2}{V_{o_2}}\ \frac{\partial V_2}{\partial V_1}\right)^2+\left(\sqrt{p_2}\ \frac{\partial \theta_2}{\partial V_1}+K\ (1-\sqrt{p_2})\ \frac{\partial \phi_2}{\partial V_1}\right)^2}$$

provided that the eccentricity is obtained from this derivative using

$$\delta e = \left(\frac{\partial e}{\partial V_1}\right) |\delta V_1|$$

rather than

$$\delta e = \left(\frac{\partial e}{\partial V_1}\right) \delta V_1 \quad .$$

As in the case of mean radius error, the eccentricity derivative can be expressed in the dimensionless form

$$V_{o_1}\ \frac{\partial e}{\partial V_1} = \sqrt{\left[2\sqrt{n}\left(\frac{\partial V_2}{\partial V_1}\right)+\frac{1}{n}\left(\frac{V_{o_1}}{r_1}\ \frac{\partial r_2}{\partial V_1}\right)\right]^2+\left[\sqrt{p_2}\left(V_{o_1}\ \frac{\partial \theta_2}{\partial V_1}\right)+K\ (1-\sqrt{p_2})\left(V_{o_1}\ \frac{\partial \phi_2}{\partial V_1}\right)\right]^2} \qquad \ldots\ (C.15)$$

and similarly

$$\frac{\partial e}{\partial \theta_1} = \sqrt{\left[2\sqrt{n}\left(\frac{1}{V_{o_1}}\ \frac{\partial V_2}{\partial \theta_1}\right)+\frac{1}{n}\left(\frac{1}{r_1}\ \frac{\partial r_2}{\partial \theta_1}\right)\right]^2+\left[\sqrt{p_2}\left(\frac{\partial \theta_2}{\partial \theta_1}\right)+K\ (1-\sqrt{p_2})\left(\frac{\partial \phi_2}{\partial \theta_1}\right)\right]^2} \qquad \ldots\ (C.16)$$

$$\left(r_1\ \frac{\partial e}{\partial r_1}\right) = \sqrt{\left[2\sqrt{n}\left(\frac{r_1}{V_{o_1}}\ \frac{\partial V_2}{\partial r_1}\right)+\frac{1}{n}\left(\frac{\partial r_2}{\partial r_1}\right)\right]^2+\left[\sqrt{p_2}\left(r_1\ \frac{\partial \theta_2}{\partial r_1}\right)+K\ (1-\sqrt{p_2})\left(r_1\ \frac{\partial \phi_2}{\partial r_1}\right)\right]^2} \qquad \ldots\ (C.17)$$

$$\frac{\partial e}{\partial \phi_1} = \sqrt{\left[2\sqrt{n}\left(\frac{1}{V_{o_1}}\ \frac{\partial V_2}{\partial \phi_1}\right)+\frac{1}{n}\left(\frac{1}{r_1}\ \frac{\partial r_2}{\partial \phi_1}\right)\right]^2+\left[\sqrt{p_2}\left(\frac{\partial \theta_2}{\partial \phi_1}\right)+K\ (1-\sqrt{p_1})\left(\frac{\partial \phi_2}{\partial \phi_1}\right)\right]^2} \quad . \qquad \ldots\ (C.18)$$

Equations (C.15) to (C.18) are plotted in Figs.15, 17, 20 and 22. It should be noted that $(\partial e/\partial \phi_1)$ for the case of the apogee impulse aligned to the local horizontal (K = 0) is zero, since the only non-zero term in equation (C.18) is $\partial \phi_2/\partial \phi_1$ (see Appendix A).

C.4 Impulsive velocities required to null mean radius and eccentricity errors of final orbit

C.4.1 Nulling radius error

Mean radius error may be nulled by application of a post injection tangential impulse. For an orbit of small eccentricity it is of no consequence at which point on the orbit the impulse is applied, and provided it is applied along the direction of motion the resulting change in mean radius is given by

$$\delta a' = \frac{2r_2}{V_{o_2}} \delta u_a \quad . \tag{C.19}$$

This formula is provided by an examination of equation (C.5). δu_a is taken here as the corrective tangential velocity and in order to null any initial error δa, $\delta a'$ must be made equal and opposite to δa.

Therefore

$$\delta u_a = \frac{V_{o_2}}{2r_2} |\delta a| \quad . \tag{C.20}$$

δa appears in the modulus sign since, for practical purposes, we are at present concerned with evaluating the magnitude of the impulsive correction rather than its vectorial value. Of course, if the initial error δe is positive δu_a must be applied in a retrograde manner, while if it is negative the required correction will be forward.

Using $\delta a = (\partial a/\partial V_1)\, \delta V_1$, for an initial velocity perturbation and substituting this in equation (C.20) we get

$$\delta u_a = \frac{V_{o_2}}{2r_2} \frac{\partial a}{\partial V_1} |\delta V_1|$$

so that

$$\delta u_a = \frac{\partial u_a}{\partial V_1} |\delta V_1| \tag{C.21}$$

where

$$\frac{\partial u_a}{\partial V_1} = \frac{V_{o_2}}{2r_2} \cdot \left|\frac{\partial a}{\partial V_1}\right| \quad . \tag{C.22}$$

We note that δu_a must be evaluated using the modulus of the input perturbation. Again, this is because we are concerned with evaluating the magnitude of the velocity correction, which is positive for either positive or negative inputs.

Equation (C.22) may be expressed in the following non-dimensional form:-

$$\boxed{\frac{\partial u_a}{\partial V_1} = \frac{1}{2n\sqrt{n}} \left| \left(\frac{V_{o_1}}{r_1} \frac{\partial a}{\partial V_1} \right) \right|} \qquad (C.23)$$

and similarly,

$$\boxed{\left(\frac{1}{V_{o_1}} \frac{\partial u_a}{\partial \theta_1} \right) = \frac{1}{2n\sqrt{n}} \left| \left(\frac{1}{r_1} \frac{\partial a}{\partial \theta_1} \right) \right|} \qquad (C.24)$$

$$\boxed{\left(\frac{r_1}{V_{o_1}} \frac{\partial u_a}{\partial r_1} \right) = \frac{1}{2n\sqrt{n}} \left| \left(\frac{\partial a}{\partial r_1} \right) \right|} \qquad (C.25)$$

$$\boxed{\frac{1}{V_{o_1}} \frac{\partial u_a}{\partial \phi_1} = \frac{1}{2n\sqrt{n}} \left| \left(\frac{1}{r_1} \frac{\partial a}{\partial \phi_1} \right) \right|} \quad . \qquad (C.26)$$

These results are plotted in Figs.16 and 21. $\partial u_a/\partial \theta_1$ and $\partial u_a/\partial \phi_1$ are both zero for all values of n.

C.4.2 Nulling eccentricity error

A tangential impulse can also be used to null a small eccentricity error. The magnitude of such an impulse, δu_e is given by

$$\delta u_e = \frac{V_{o_2}}{2} \delta e \quad . \qquad (C.27)$$

This result is seen from equation (C.6). It is interesting to note that if eccentricity error was corrected by a vertical impulse, rather than a tangential one, the velocity required would be twice as large, since $\delta\theta$ = vertical velocity/V_{o_2}. Eccentricity error can be reduced by either a forward impulse at apogee or a retrograde impulse at perigee.

From equation (C.27) we can see that

$$\frac{\partial u_e}{\partial V_1} = \frac{\partial e}{\partial V_1} \cdot \frac{V_{o_2}}{2} \quad . \tag{C.28}$$

Again we must remember to evaluate δu_e from the relation

$$\delta u_e = \frac{\partial u_e}{\partial V_1} |\delta V_1|$$

rather than

$$\delta u_e = \frac{\partial u_e}{\partial V_1} \delta V_1 \quad .$$

Equation (C.28) can be expressed in the non-dimensional form:-

$$\boxed{\frac{\partial u_e}{\partial V_1} = \frac{1}{2\sqrt{n}} \left(V_{o_1} \frac{\partial e}{\partial V_1} \right)} \tag{C.29}$$

and similarly,

$$\boxed{\left(\frac{1}{V_{o_1}} \frac{\partial u_e}{\partial \theta_1} \right) = \frac{1}{2\sqrt{n}} \left(\frac{\partial e}{\partial \theta_1} \right)} \tag{C.30}$$

$$\boxed{\left(\frac{r_1}{V_{o_1}} \frac{\partial u_e}{\partial r_1} \right) = \frac{1}{2\sqrt{n}} \left(r_1 \frac{\partial e}{\partial r_1} \right)} \tag{C.31}$$

$$\boxed{\left(\frac{1}{V_{o_1}} \frac{\partial u_e}{\partial \phi_1} \right) = \frac{1}{2\sqrt{n}} \left(\frac{\partial e}{\partial \phi_1} \right)} \quad . \tag{C.32}$$

It should be noted that there is no need to include a modulus sign on the right hand side of equations (C.29) to (C.32), since eccentricity derivatives are already positive. These derivatives are plotted in Figs.16, 18, 21 and 23.

C.4.3 Simultaneous nulling of radius and eccentricity errors

In general this type of correction will require two tangential impulses δu_1 and δu_2 (see Fig.10). The impulses must be allocated in such a manner that:

(i) the algebraic sum (taking into account whether the impulses are forward or retrograde) must null the radius error,

(ii) the two impulses must be split between apogee and perigee so that the nett eccentricity correction equals the initial eccentricity error.

In Fig.10(a) the perturbed orbit lies wholly outside the desired circular orbit and hence both impulses are retrograde (or forward). Thus the total impulse requirement in this case is dictated by radius correction and the eccentricity correction can be accommodated within this requirement.

In the other case (Fig.10(b)) the perturbed orbit intercepts the desired one, and both impulses are instrumental in nulling eccentricity. Thus the total requirement is dictated by the initial eccentricity and mean radius correction can be accommodated within this requirement.

The condition that the perturbed ellipse does not intercept the desired one is that

$$r_2 (1-\delta e) + \delta a > r_2$$

or

$$r_2 (1+\delta e) + \delta a < r_2$$

i.e.

$$|\delta a| > r_2 \, \delta e \quad . \tag{C.33}$$

Comparison of this equation with equations (C.20) and (C.27) shows that this is equivalent to the condition

$$\delta u_a > \delta u_e$$

as would be expected.

To summarise we can suppose that in general δu_a can be either greater or less than δu_e, depending upon the nature of the perturbed orbit. Both mean radius and eccentricity errors can be nulled by application of two tangential impulses whose arithmetical sum equals the larger of δu_e and δu_a, provided the impulses are applied at the correct places.

It will be seen by examining the curves of Figs.16, 18, 21 and 23 that δu_e may indeed be larger or smaller than δu_a, depending upon the nature of the perturbation.

Table 1(a)

FORMULAE FOR DERIVATIVES RELATING POSITION AND VELOCITY ERRORS AT START OF TRANSFER TO THOSE AT END – POLAR CO-ORDINATE SYSTEM

$\frac{\partial V_2}{\partial V_1} = -\left(2 + \frac{1}{n}\right)$	$V_{o_1} \frac{\partial \theta_2}{\partial V_1} = \frac{3\pi}{4\sqrt{2}} (1+n)^{3/2} \left(1 - \frac{1}{n}\right)$	$\frac{V_{o_1}}{r_1} \frac{\partial r_2}{\partial V_1} = \sqrt{2n(1+n)^3}$	$V_{o_1} \frac{\partial \phi_2}{\partial V_1} = -\frac{3\pi}{4n}\sqrt{2(1+n)^3}$
$\frac{1}{V_{o_1}} \frac{\partial V_2}{\partial \theta_1} = 0$	$\frac{\partial \theta_2}{\partial \theta_1} = -\frac{1}{n}$	$\frac{1}{r_1} \frac{\partial r_2}{\partial \theta_1} = 0$	$\frac{\partial \phi_2}{\partial \theta_1} = -2\left(1 + \frac{1}{n}\right)$
$\frac{r_1}{V_{o_1}} \frac{\partial V_2}{\partial r_1} = -\sqrt{2\left(1 + \frac{1}{n}\right)}$	$r_1 \frac{\partial \theta_2}{\partial r_1} = \frac{3\pi}{8n\sqrt{n}} (n-1)(n+1)^2$	$\frac{\partial r_2}{\partial r_1} = n(n+2)$	$r_1 \frac{\partial \phi_2}{\partial r_1} = -\frac{3\pi}{4n\sqrt{n}} (1+n)^2$
$\frac{1}{V_{o_1}} \frac{\partial V_2}{\partial \phi_1} = 0$	$\frac{\partial \theta_2}{\partial \phi_1} = 0$	$\frac{1}{r_1} \cdot \frac{\partial r_2}{\partial \phi_1} = 0$	$\frac{\partial \phi_2}{\partial \phi_1} = 1$

Table 1(b)

CORRESPONDING DERIVATIVES IN CARTESIAN CO-ORDINATE SYSTEM

$\frac{\partial x_2^o}{\partial x_1^o} = 2 + \frac{1}{n}$	$\frac{\partial z_2^o}{\partial x_1^o} = -\frac{3\pi}{4n\sqrt{n}}(1+n)^2$	$\frac{V_{o_1}}{r_1}\frac{\partial x_2}{\partial x_1^o} = \frac{3\pi}{4}\sqrt{2(1+n)^3}$	$\frac{V_{o_1}}{r_1}\frac{\partial z_2}{\partial x_1^o} = -\sqrt{2n(1+n)^3}$
$\frac{\partial x_2^o}{\partial z_1^o} = 0$	$\frac{\partial z_2^o}{\partial z_1^o} = -\frac{(1+2n)}{n^2}$	$\frac{V_{o_1}}{r_1}\frac{\partial x_2}{\partial z_1^o} = \sqrt{\frac{2(1+n)^3}{n}}$	$\frac{V_{o_1}}{r_1}\frac{\partial z_2}{\partial z_1^o} = 0$
$\frac{r_1}{V_{o_1}}\frac{\partial x_2^o}{\partial x_1} = 0$	$\frac{r_1}{V_{o_1}}\cdot\frac{\partial z_2^o}{\partial x_1} = -\sqrt{\frac{2(1+n)}{n^3}}$	$\frac{\partial x_2}{\partial x_1} = n+2$	$\frac{\partial z_2}{\partial x_1} = 0$
$\frac{r_1}{V_{o_1}}\frac{\partial x_2^o}{\partial z_1} = \sqrt{2\left(1+\frac{1}{n}\right)}$	$\frac{r_1}{V_{o_1}}\frac{\partial z_2^o}{\partial z_1} = -\frac{3\pi}{4\sqrt{2n^2}}(1+n)^{5/2}$	$\frac{\partial x_2}{\partial z_1} = \frac{3\pi}{4\sqrt{n}}(1+n)^2$	$\frac{\partial z_2}{\partial z_1} = -n(n+2)$

SYMBOLS

a	mean radius of orbit
e	eccentricity
K	coefficient defining method of alignment of apogee impulse
$n = \frac{r_2}{r_1}$	transfer ratio
$p = \frac{rV^2}{\mu}$	dimensionless parameter relating speed to circular orbital speed
r	geocentric radius
T_o	orbital period of transfer orbit
δu_a	magnitude of post-orbital velocity correction required to null mean radius error
δu_e	magnitude of post-orbital velocity correction required to null eccentricity error
V	velocity magnitude
$V_o = \sqrt{\mu/r}$	circular orbital speed at radius r
x, z	cartesian position co-ordinates
θ	flight path angle relative to local horizontal
ϕ	angular range
μ	earth's gravitational constant

Subscripts:-

1	point at which Hohmann transfer starts
2	point at which Hohmann transfer ends

REFERENCES

No.	Author	Title, etc.
1	W. Hohmann	Die Erreichbarkeit der Himmelskörper (Oldenbaurg, Munich 1925) (Translated as NASA TT F-44, 1960)
2	D.G. King-Hele	An introduction to transfer orbits. RAE Tech. Note No. Space 17, 1962
3	-	ELDO Future Programmes Preliminary Study 1.1. RAE Space Dept. Paper Ref. RAE/SPA/L/C.917, 1964
4	G.B. Longden	Optimum vacuum ballistic trajectories over a non-rotating earth. RAE Tech. Note No. GW.366, 1955
5	R. Law	The effects of injection errors on a satellite orbit. RAE Tech. Note No. Space 45/WE.37, 1963
6	-	Design guide to orbital flight. (McGraw-Hill, New York, 1962)
7	B.A.C. (Editor)	ELDO Apogee Stage. ELDO Future Programmes. Project No.1. Study No.1.5 (U.K. Study) 1965

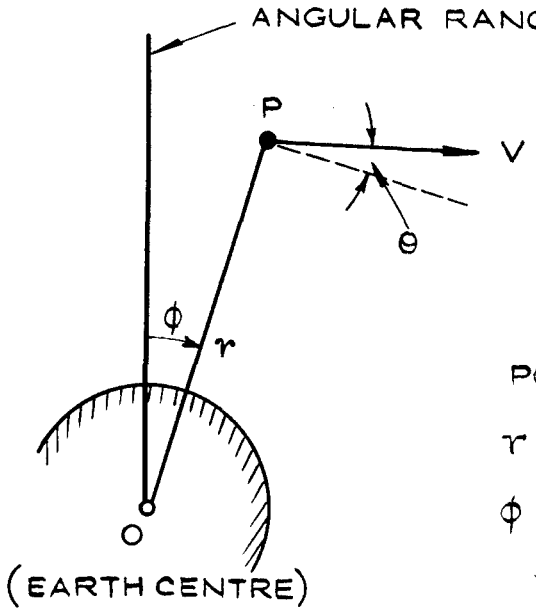

(a) POLAR

POSITION CO-ORDINATES:-

r GEOCENTRIC RADIUS

ϕ ANGULAR RANGE

VELOCITY CO-ORDINATES

V VELOCITY MAGNITUDE

θ CLIMB PATH ANGLE RELATIVE TO LOCAL HORIZONTAL

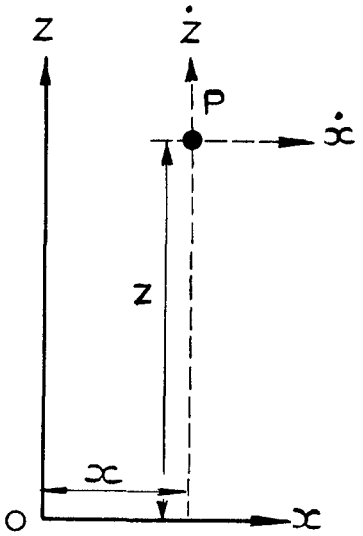

(b) CARTESIAN

POSITION CO-ORDINATES:-

x, z.

VELOCITY CO-ORDINATES:-

$\dot{x}$, $\dot{z}$

FIG.1 (a&b) TWO DIMENSIONAL CO-ORDINATE SYSTEMS

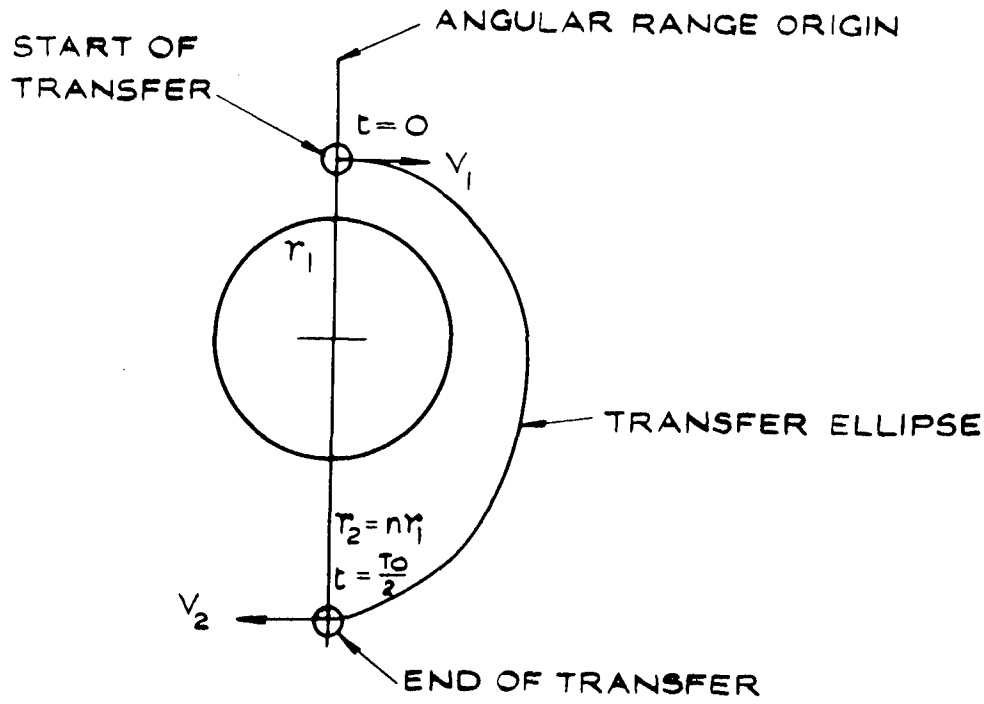

INITIAL CONDITIONS

$t = 0$

$r = r_1$

$\phi = \phi_1 = 0$

$V = V_1 = V_{0_1}\sqrt{\frac{2n}{n+1}} = V_{0_1}\sqrt{p_1}$

$\theta = \theta_1 = 0$

TERMINAL CONDITIONS

$t = \frac{T_0}{2} = \pi\sqrt{\frac{(r_1+r_2)^3}{8\mu}}$

$r = r_2 = n r_1$

$\phi = \phi_2 = \pi$

$V = V_2 = V_{0_1}\sqrt{\frac{2}{n(n+1)}} = V_{0_2}\sqrt{\frac{2}{n+1}} = V_{0_2}\sqrt{p_2}$

$\theta = \theta_2 = 0$

$\left(V_{0_1} = \sqrt{\frac{\mu}{r_1}}\quad, V_{0_2} = \sqrt{\frac{\mu}{r_2}} = \frac{V_{0_1}}{\sqrt{n}}\right)$

(V_{0_1} IS CIRCULAR ORBITAL SPEED AT RADIUS r_1)

FIG.2 CONDITIONS AT START AND END OF HOHMANN TRANSFER (POLAR SYSTEM)

Fig.3

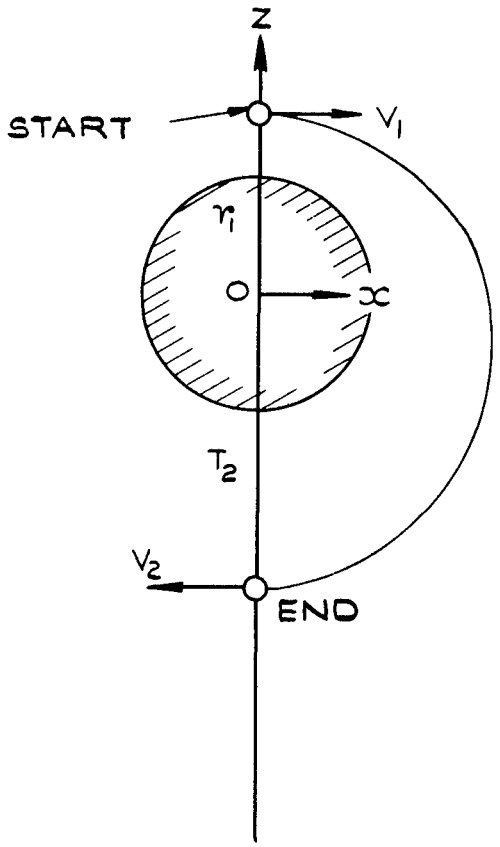

INITIAL CONDITIONS

$$t = 0$$
$$x = x_1 = 0$$
$$z = z_1 = r_1$$
$$\dot{x} = \mathring{x}_1 = V_1$$
$$\dot{z} = \mathring{z}_1 = 0$$

TERMINAL CONDITIONS

$$t = \frac{T_0}{2}$$
$$x = x_2 = 0$$
$$z = z_2 = -r_2$$
$$\dot{x} = \mathring{x}_2 = -V_2$$
$$\dot{z} = \mathring{z}_2 = 0$$

FIG. 3 CONDITIONS AT START AND END OF HOHMANN TRANSFER (CARTESIAN SYSTEM)

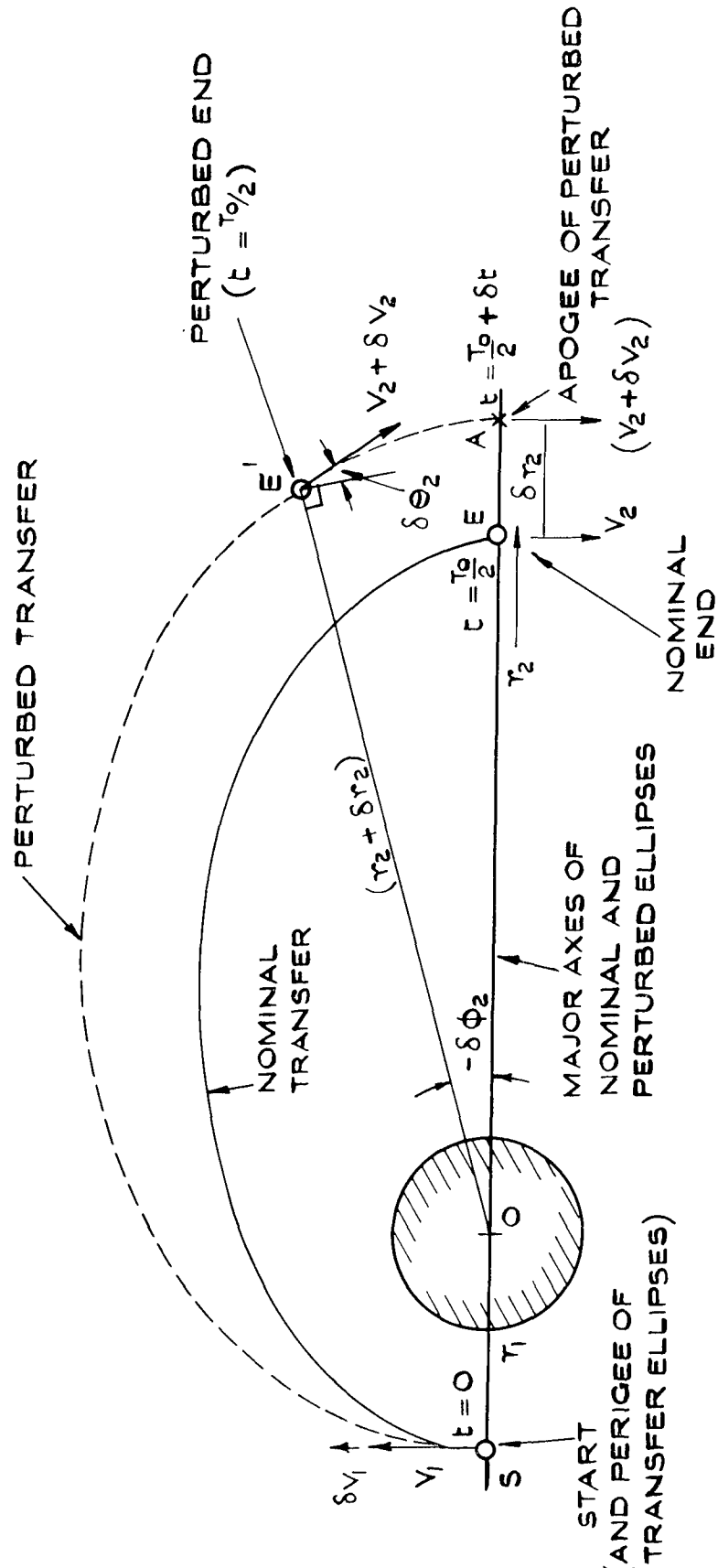

FIG. 4 EFFECT OF INITIAL v PERTURBATION ON CONDITIONS AT END OF TRANSFER

Fig.5

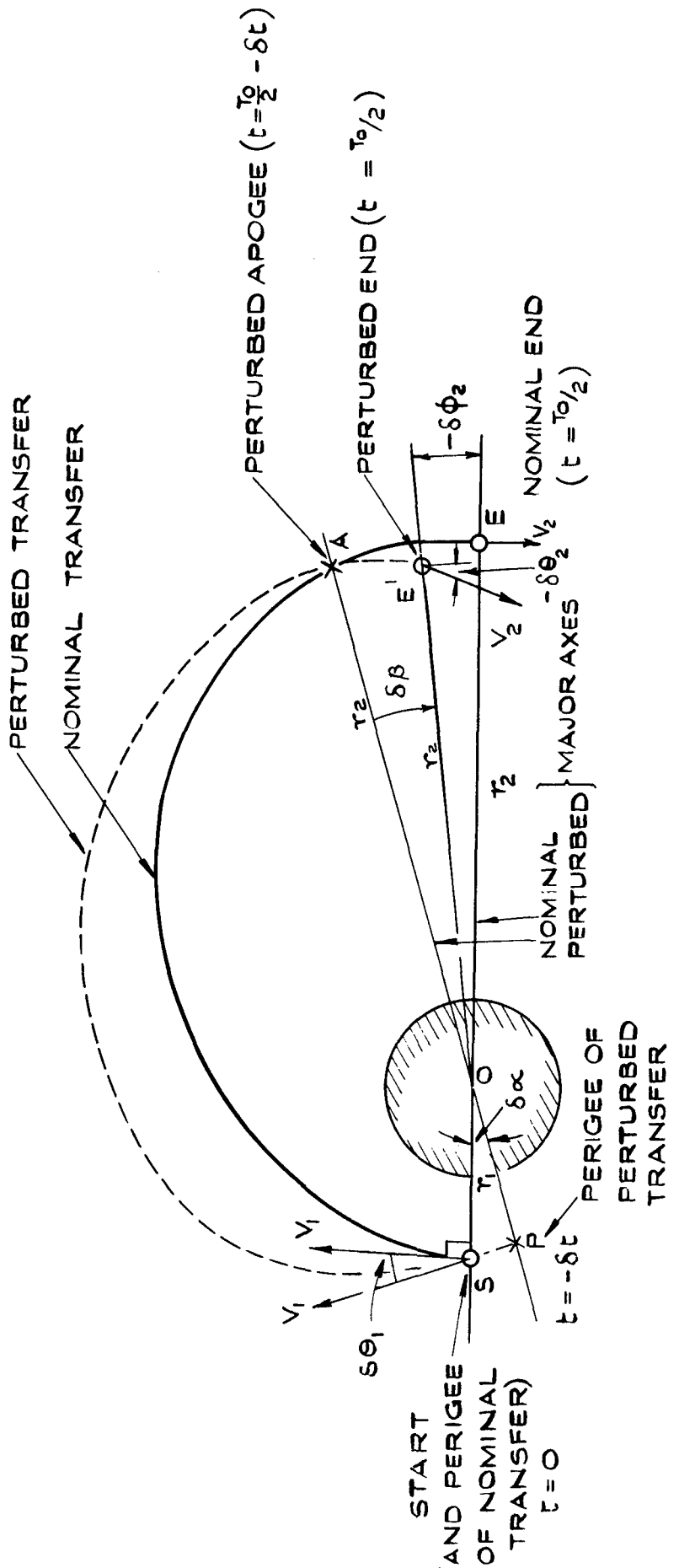

FIG. 5 EFFECT OF INITIAL Θ PERTURBATION ON CONDITIONS AT END OF TRANSFER

Fig.6

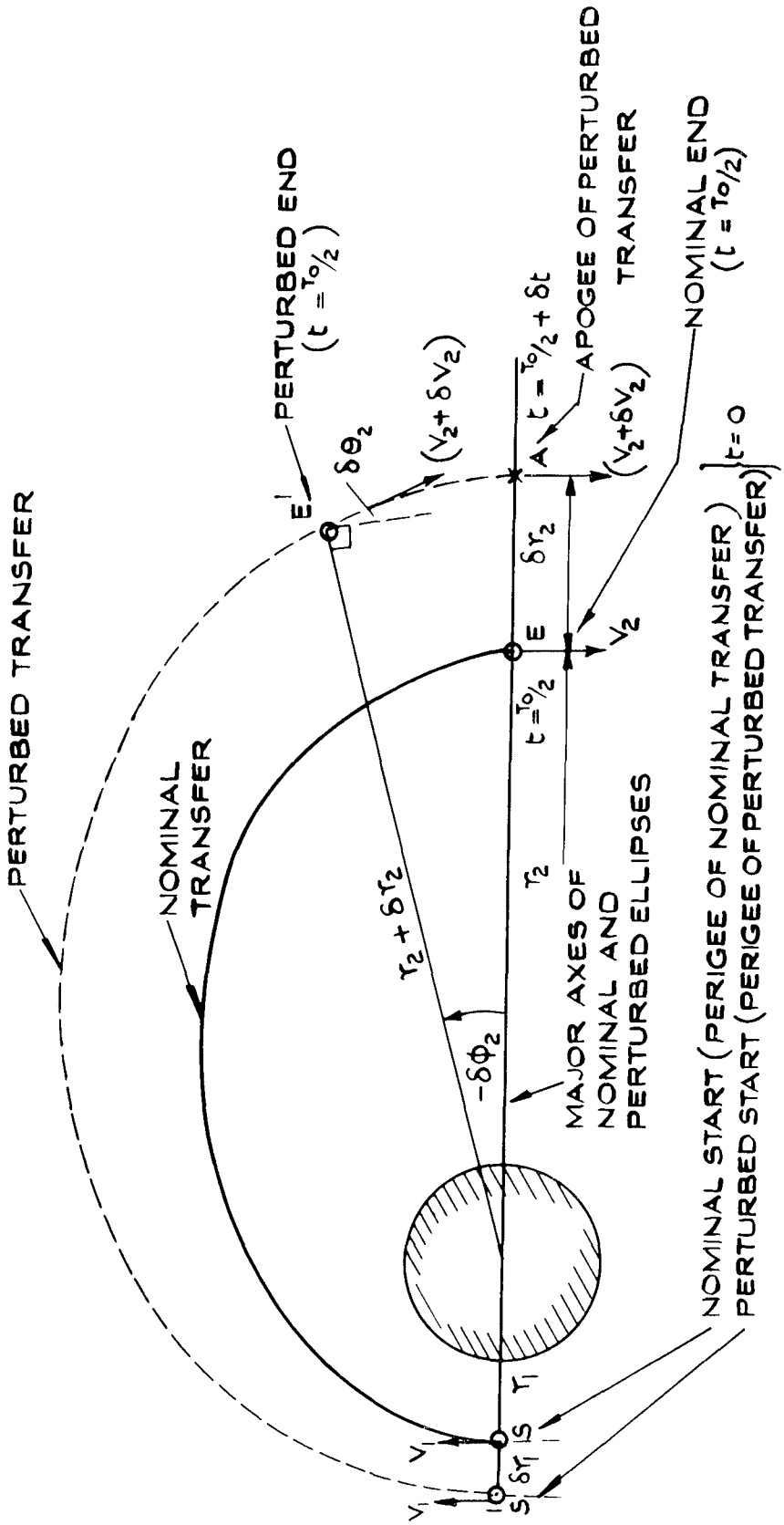

FIG. 6 EFFECT OF INITIAL τ PERTURBATION ON CONDITIONS AT END OF TRANSFER

Fig.7

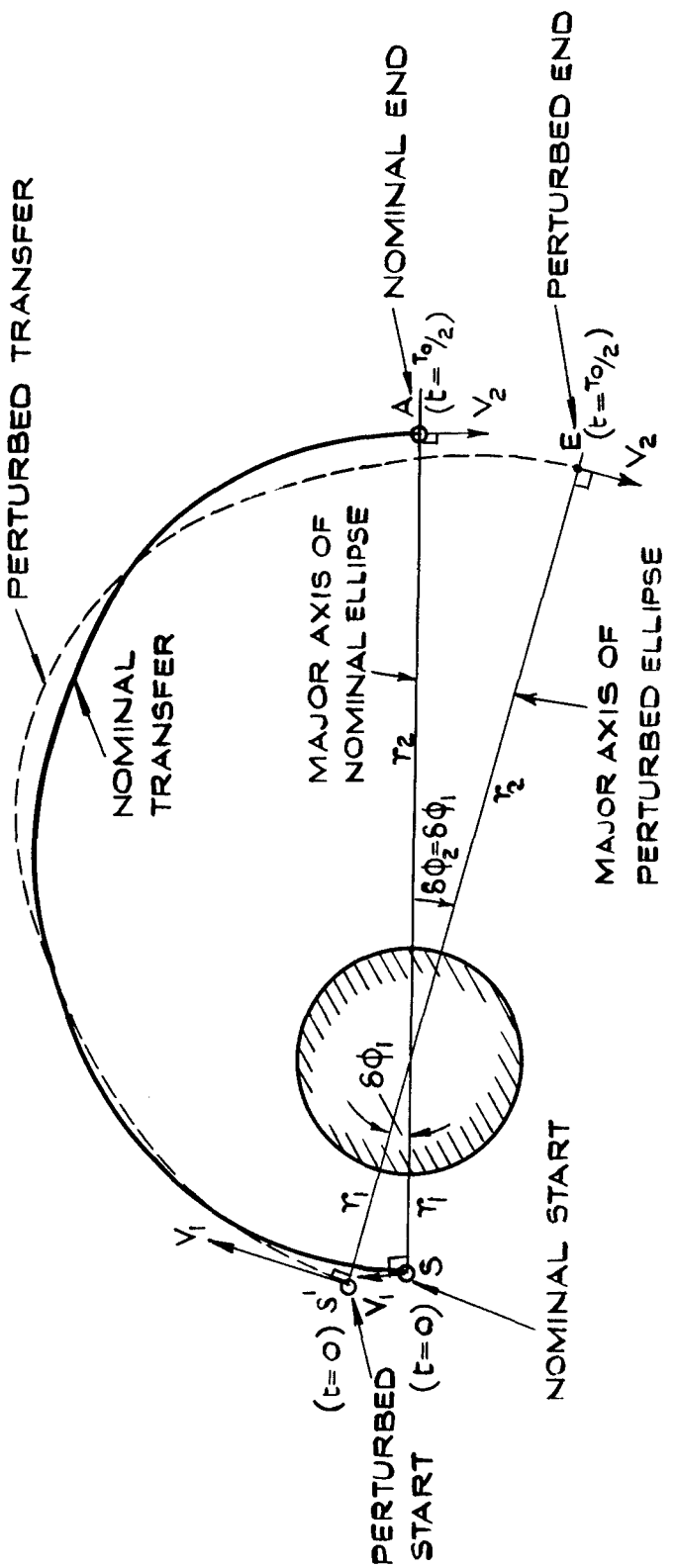

FIG. 7 EFFECT OF INITIAL ϕ PERTURBATION ON CONDITIONS AT END OF TRANSFER

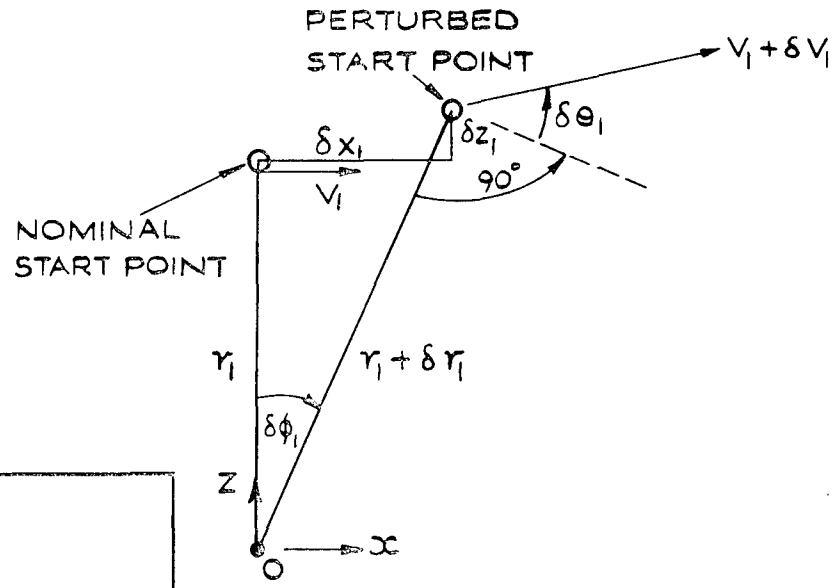

$$\delta r_1 = \delta z_1$$
$$\delta\phi_1 = \frac{1}{r_1}\,\delta x_1$$
$$\delta V_1 = \delta \dot{x}_1$$
$$\delta\theta_1 = \frac{1}{V_1}\,\delta \dot{z}_1 + \frac{1}{r_1}\,\delta x_1$$

(a) START

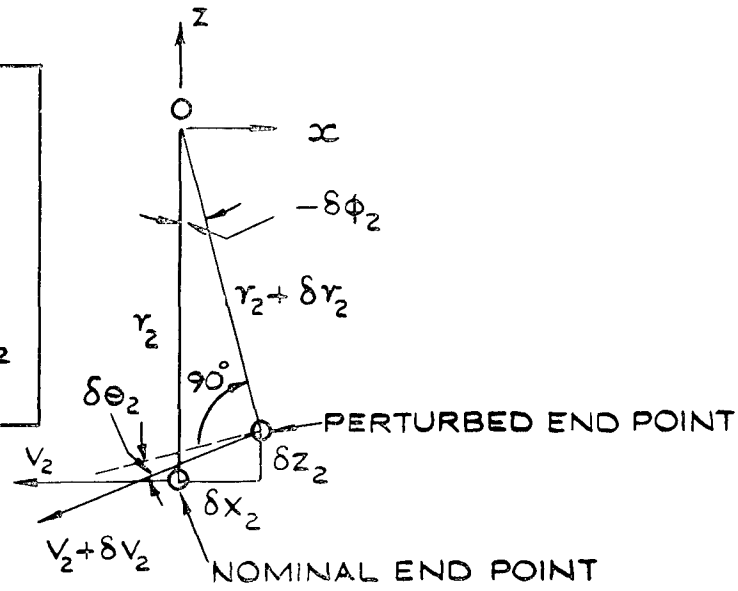

$$\delta x_2 = -r_2\,\delta\phi_2$$
$$\delta z_2 = -\delta r_2$$
$$\delta \dot{x}_2 = -\delta V_2$$
$$\delta z_2 = -V_2\,\delta\theta_2 + V_2\,\delta\phi_2$$

(b) END

FIG. 8 (a&b) RELATION BEWEEN POLAR AND CARTESIAN PERTURBATIONS AT START AND END OF TRANSFER

Fig.9

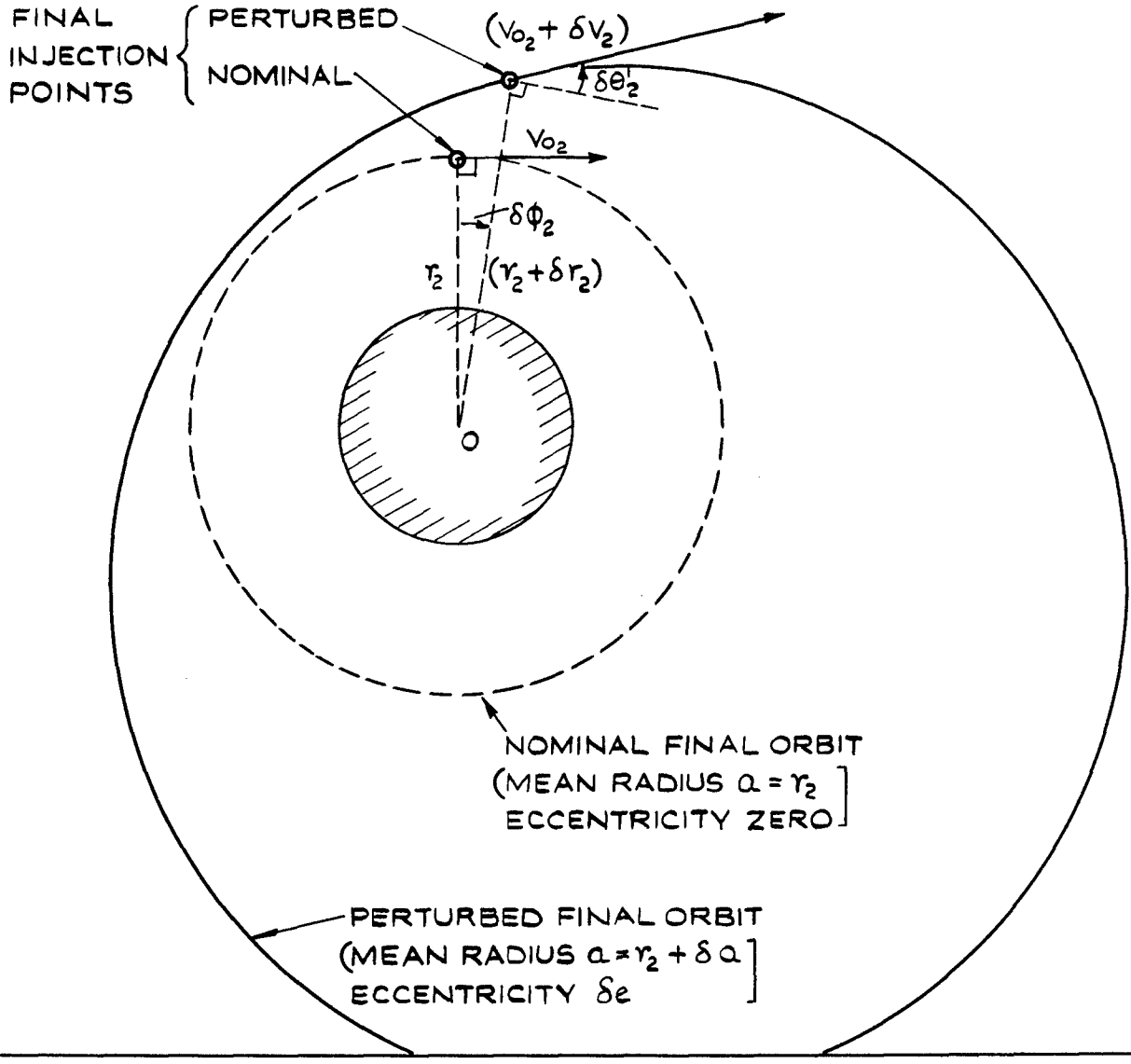

VECTOR ADDITION OF VELOCITIES AT FINAL INJECTION POINT	(1) VELOCITY AT END OF TRANSFER (2) VELOCITY ADDED BY IMPULSE (3) VELOCITY AT FINAL INJECTION
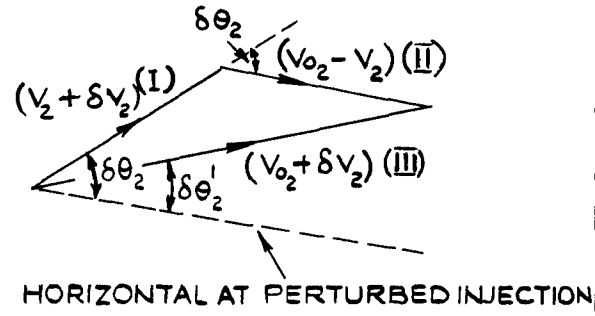	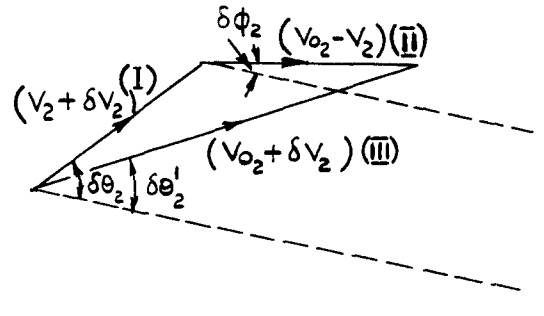
K = 0 CASE IN WHICH APOGEE IMPULSE IS ALIGNED TO LOCAL HORIZONTAL	K = 1 CASE IN WHICH APOGEE IMPULSE IS ALIGNED INSPACE (DIRECTION OF HORIZONTAL AT NOMINAL INJECTION)

FIG. 9 CONTRIBUTIONS TO ERRORS IN FINAL CIRCULAR ORBIT

Fig.10

SPA/P/1632

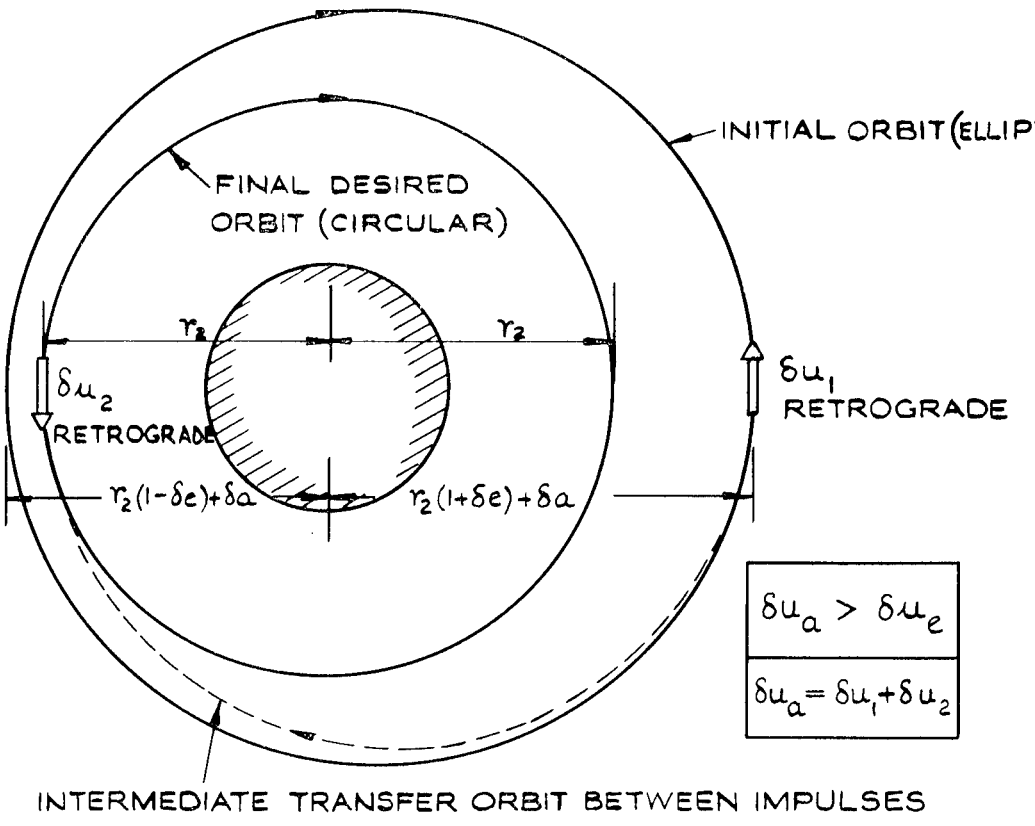

(a) CASE IN WHICH INITIAL ORBIT DOES NOT INTERCEPT FINAL ORBIT

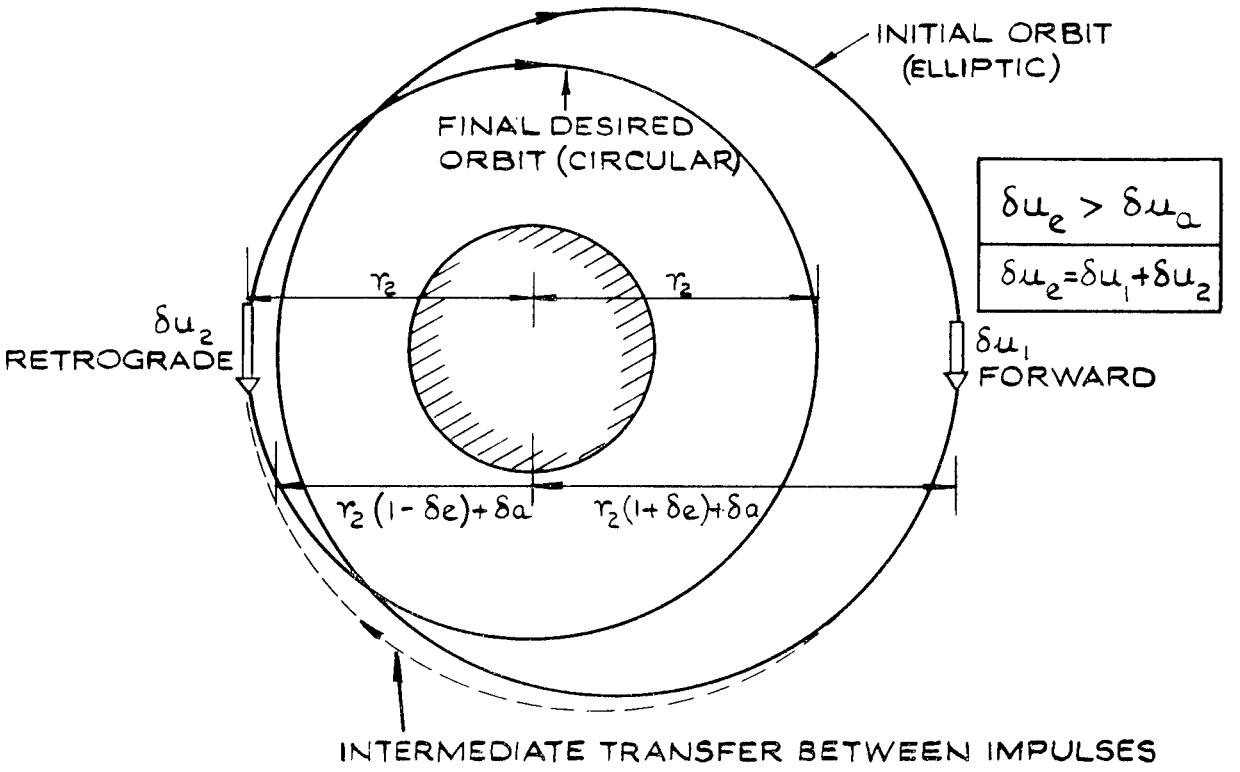

(b) CASE IN WHICH INITIAL ORBIT INTERCEPTS FINAL ORBIT

FIG 10(a & b) SIMULTANEOUS NULLING OF MEAN RADIUS AND ECCENTRICITY ERRORS BY MEANS OF TWO TANGENTIAL IMPULSES

Fig.11

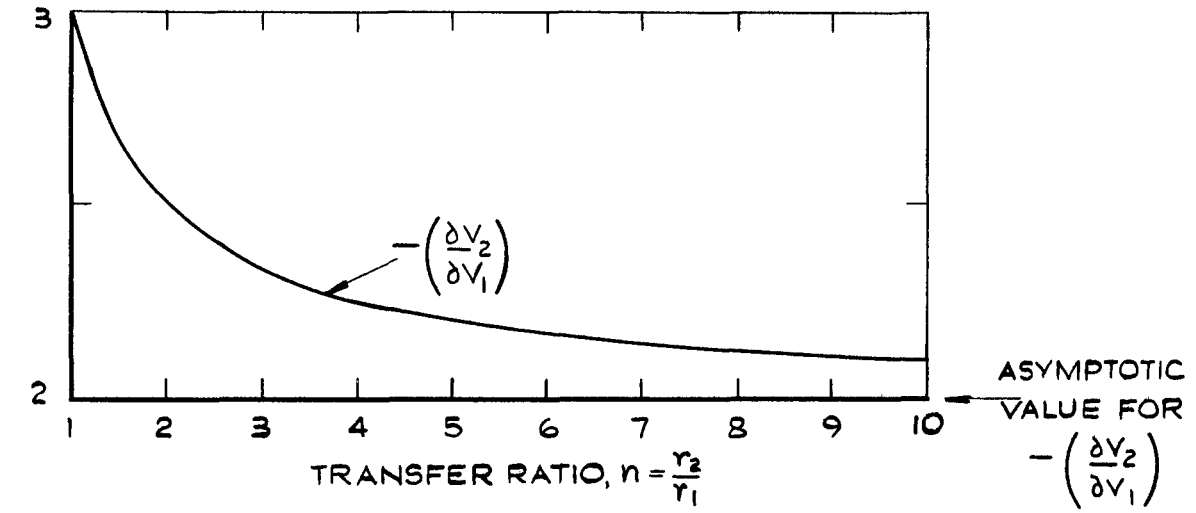

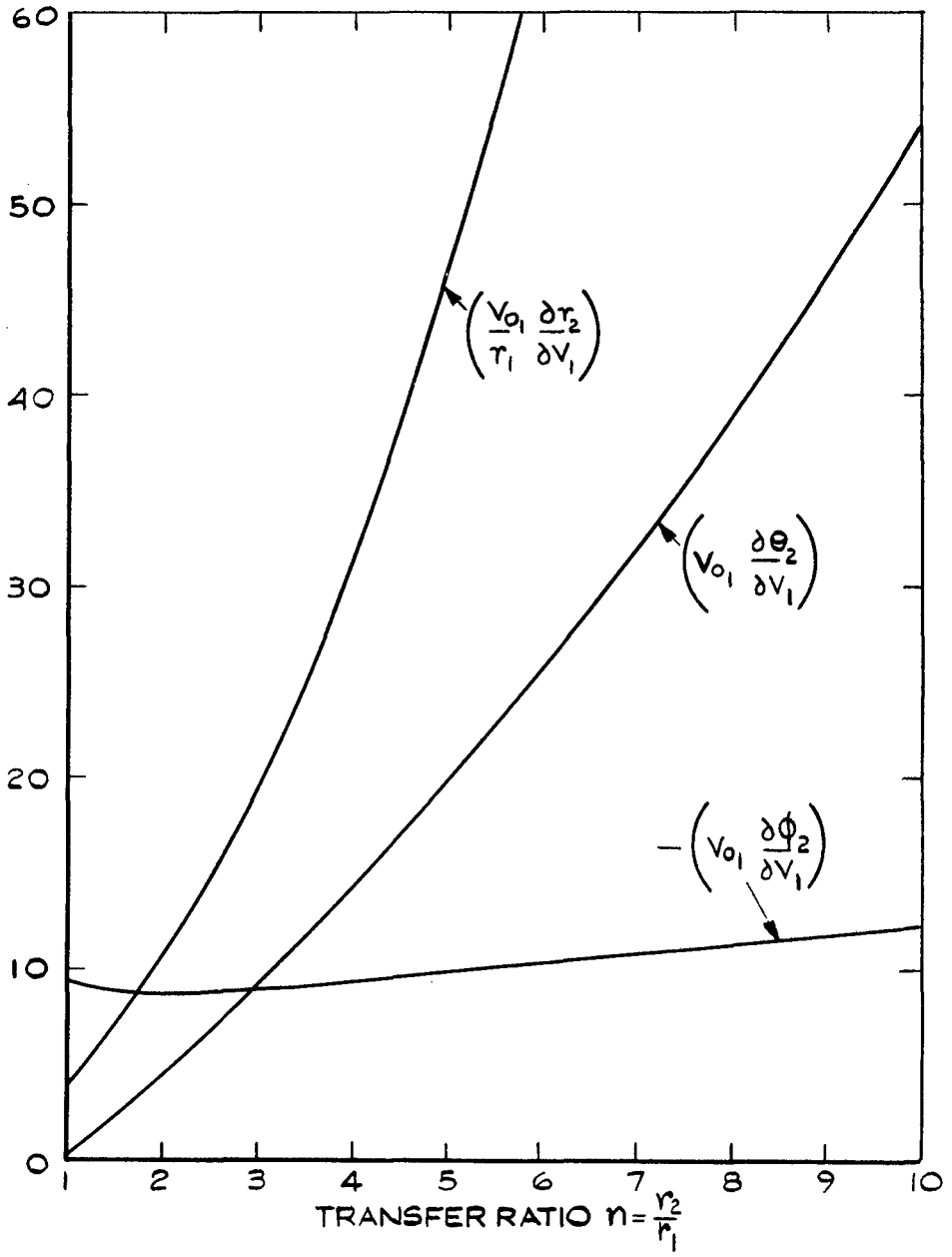

FIG.11 DERIVATIVES RELATING POSITION & VELOCITY ERRORS AT END OF TRANSFER DUE TO VELOCITY ERROR δV_1 AT START

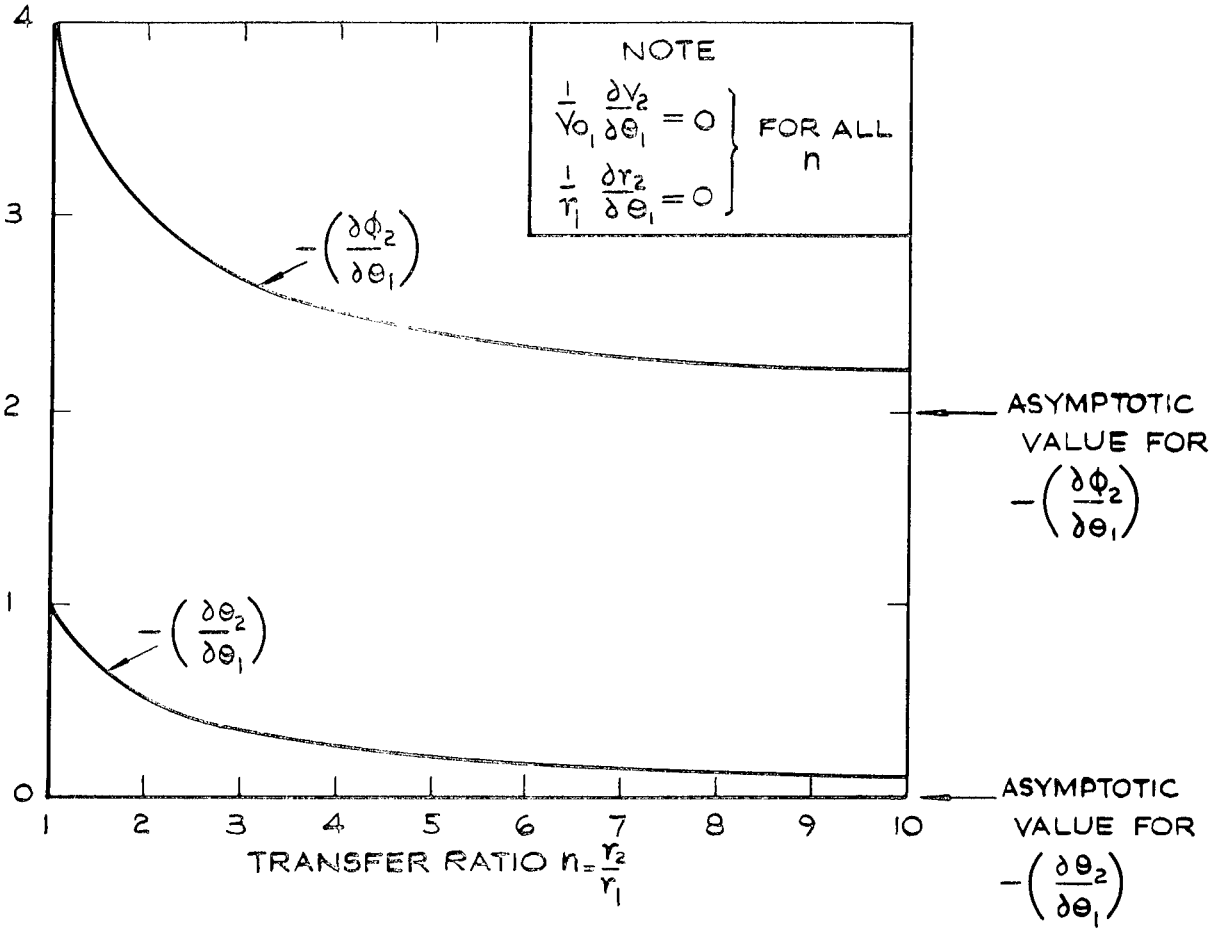

FIG.12 DERIVATIVES RELATING POSITION AND VELOCITY ERRORS AT END OF TRANSFER DUE TO CLIMB ANGLE ERROR $\delta\theta_1$ AT START

Fig.13

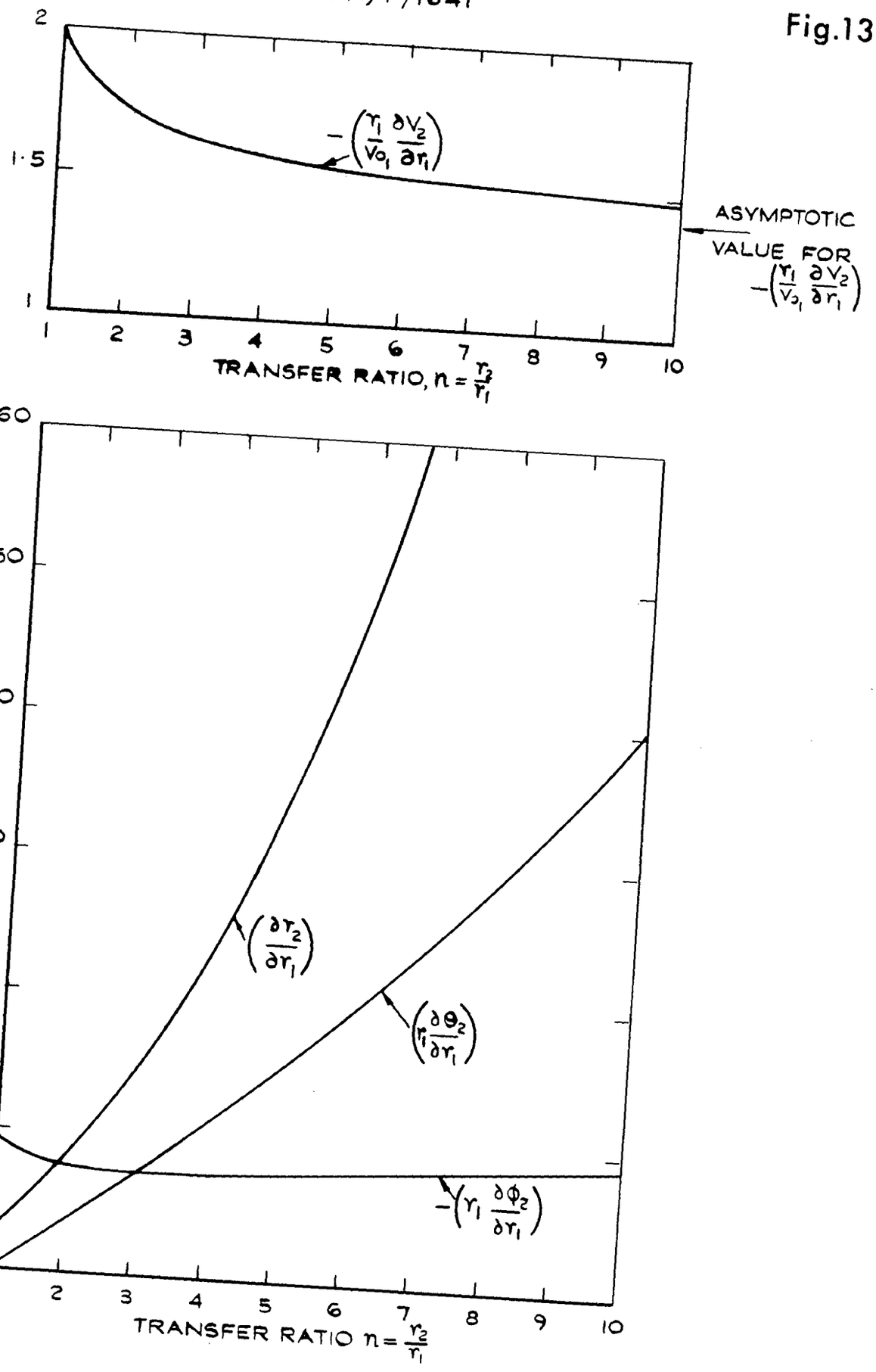

FIG.13 DERIVATIVES RELATING POSITION & VELOCITY ERRORS AT END OF TRANSFER DUE TO RADIAL POSITION ERROR ∂r_1 AT START

Fig.14

SPA/P/1642

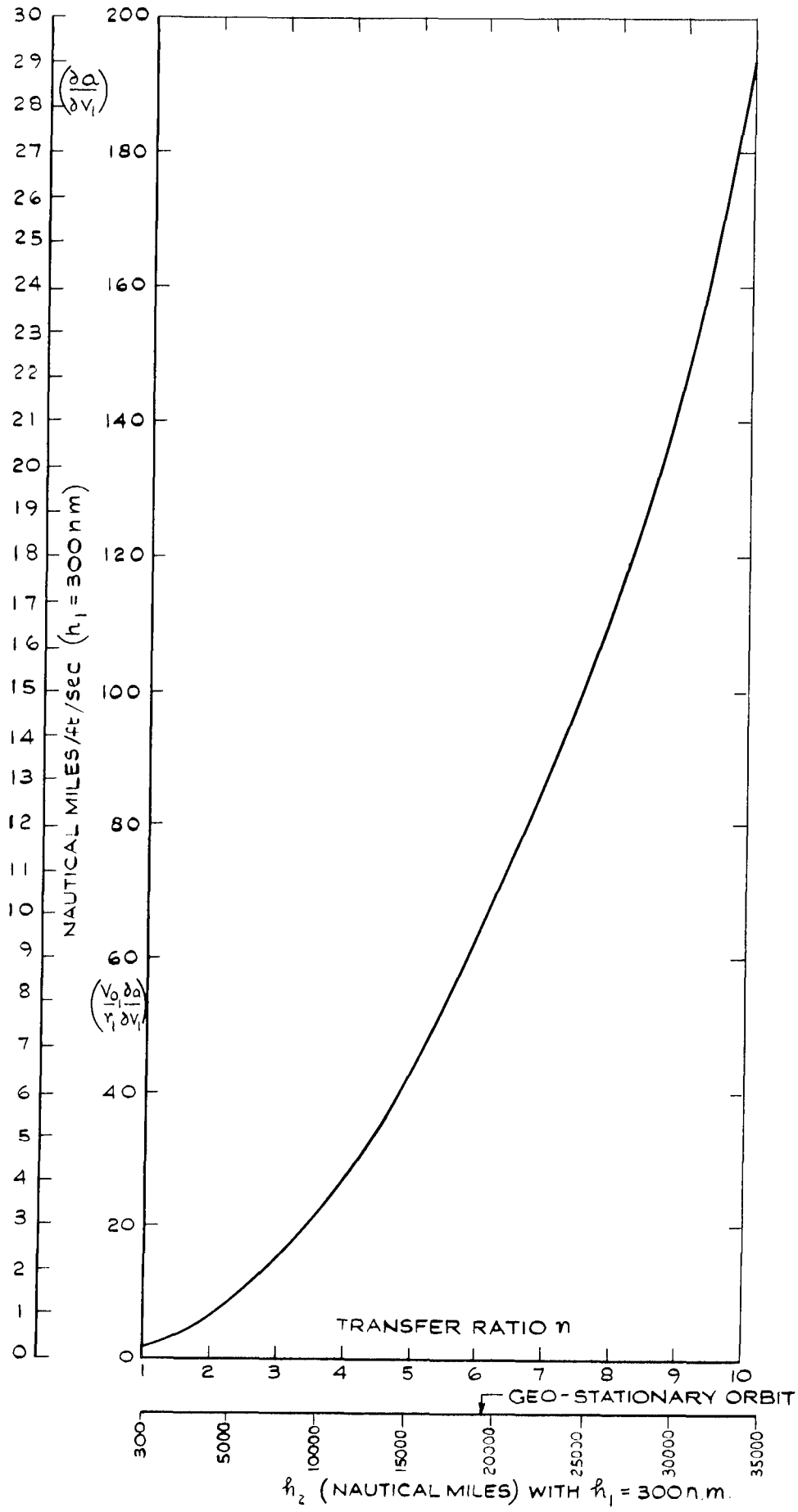

FIG.14 MEAN RADIUS ERROR OF FINAL ORBIT, DUE TO VELOCITY ERROR δV_1 AT START OF TRANSFER

Fig.15

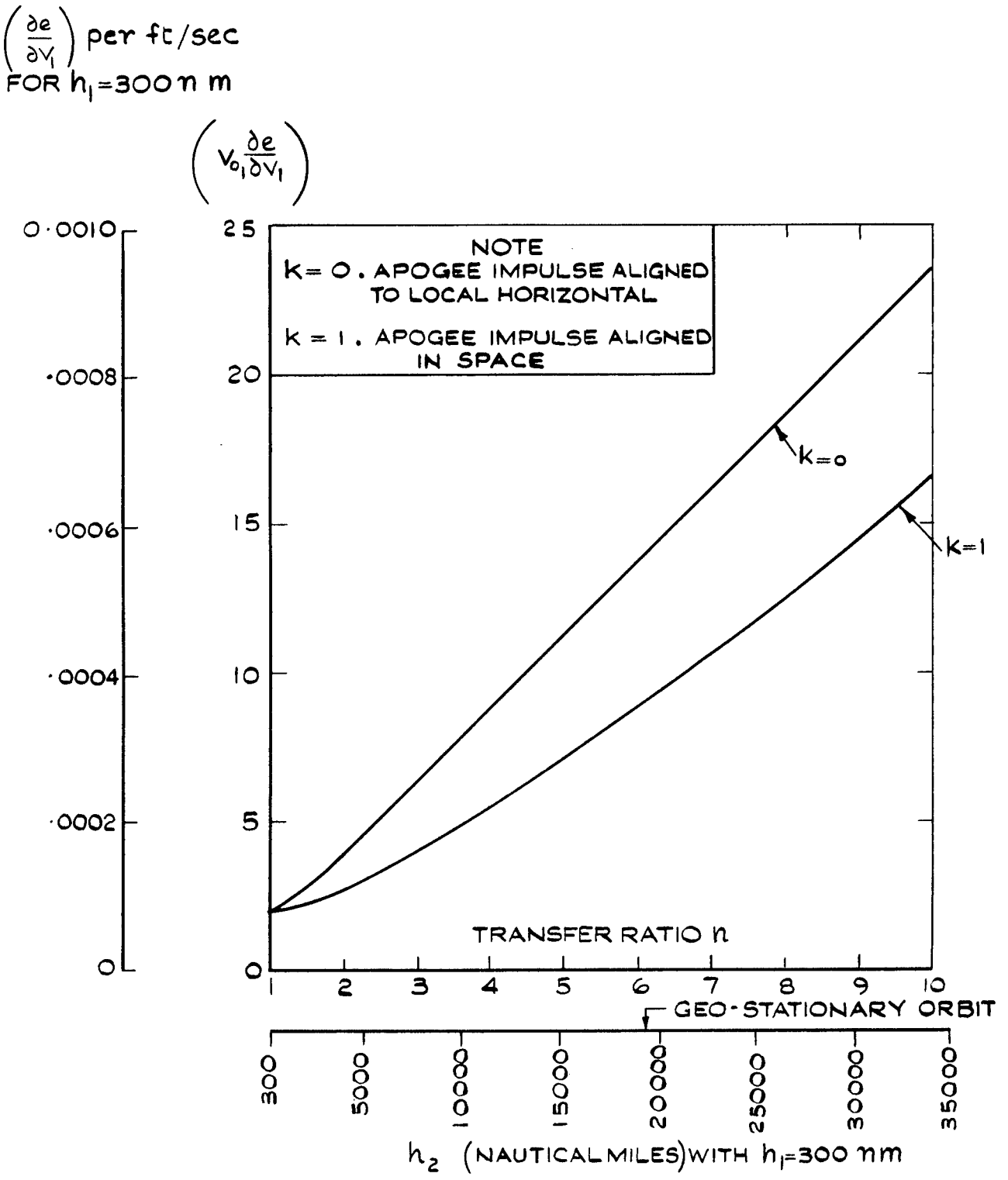

FIG.15 ECCENTRICITY OF FINAL ORBIT, DUE TO VELOCITY ERROR δV_1 AT START OF TRANSFER

Fig.16

SPA/P/1644

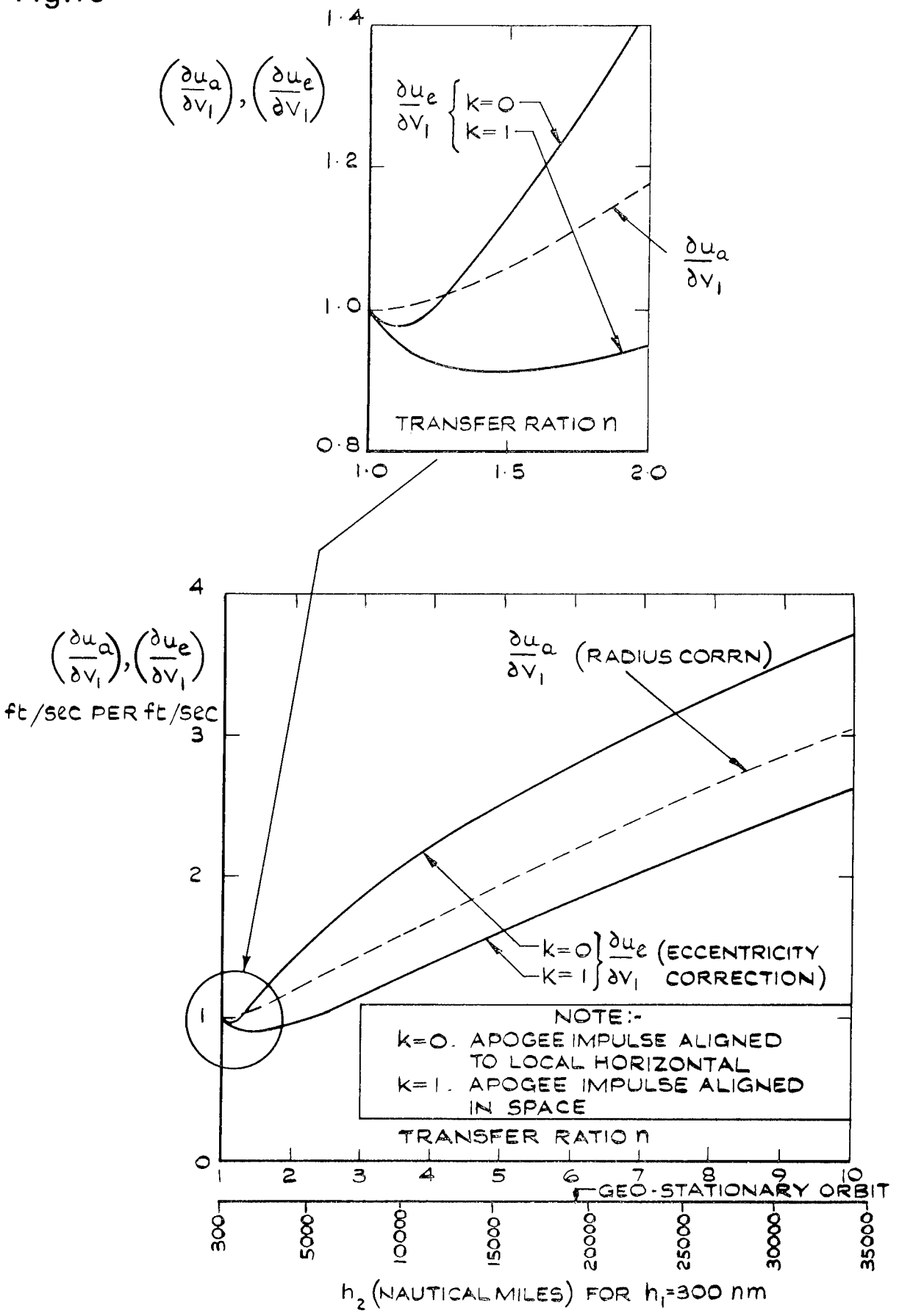

FIG.16 VELOCITIES REQUIRED TO CORRECT MEAN RADIUS & ECCENTRICITY ERRORS OF FINAL ORBIT, DUE TO VELOCITY ERROR δV_1 AT START OF TRANSFER

Fig.17

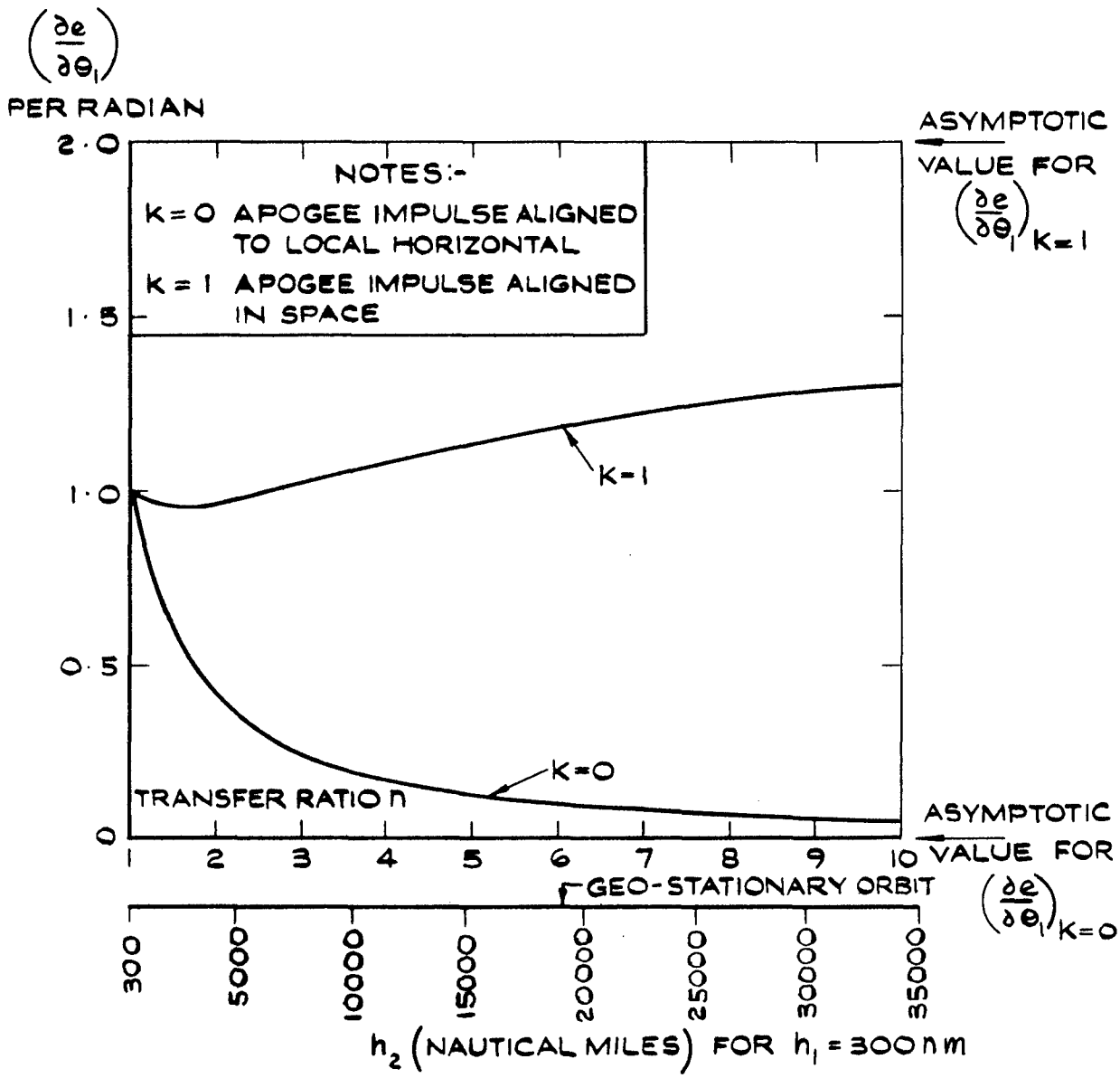

FIG.17 ECCENTRICITY OF FINAL ORBIT DUE TO CLIMB ANGLE ERROR $\delta\theta_1$ AT START OF TRANSFER

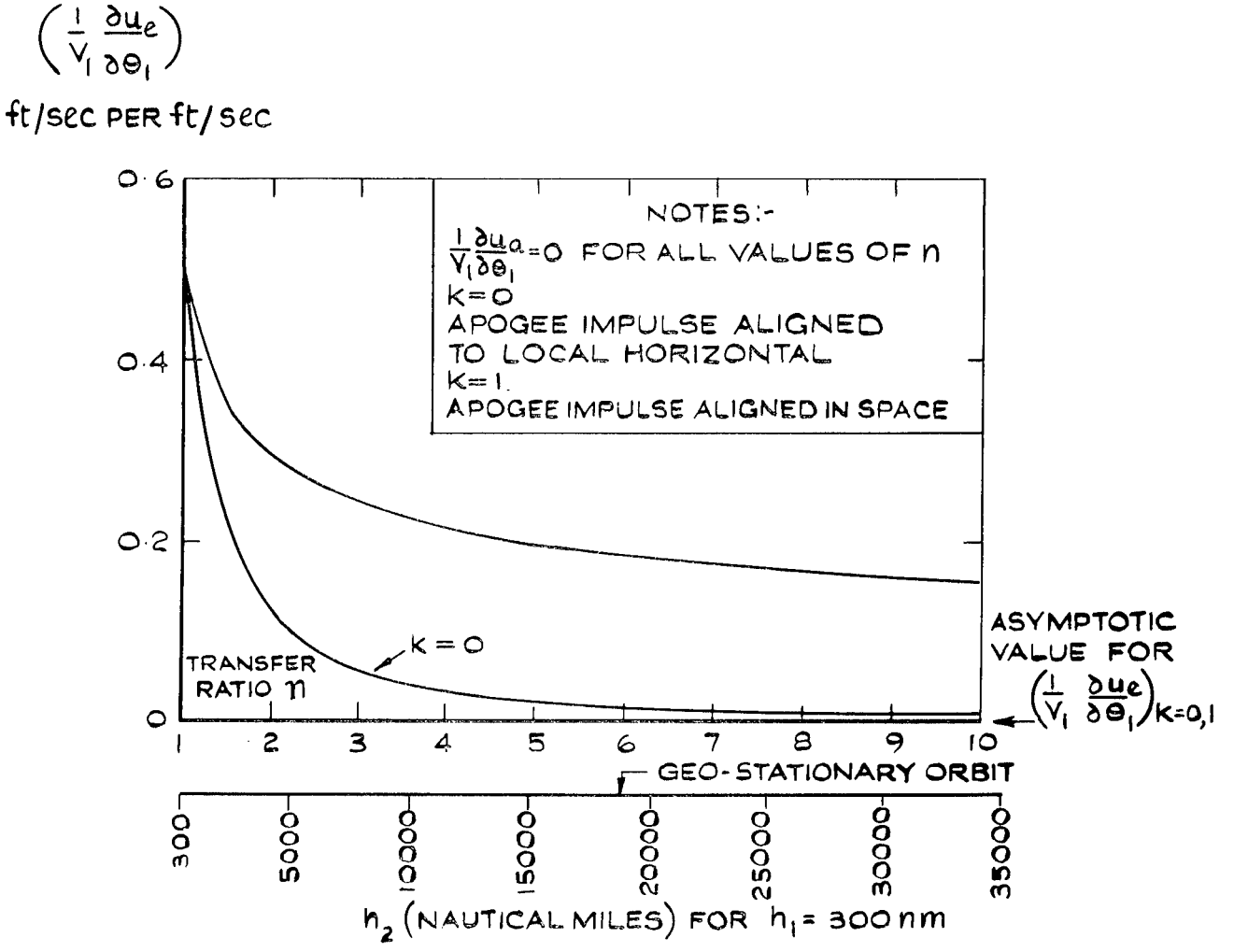

FIG.18 VELOCITY REQUIRED TO CORRECT ECCENTRICITY ERROR, DUE TO VERTICAL VELOCITY ERROR $V_1\delta\theta_1$ AT START OF TRANSFER

Fig.19

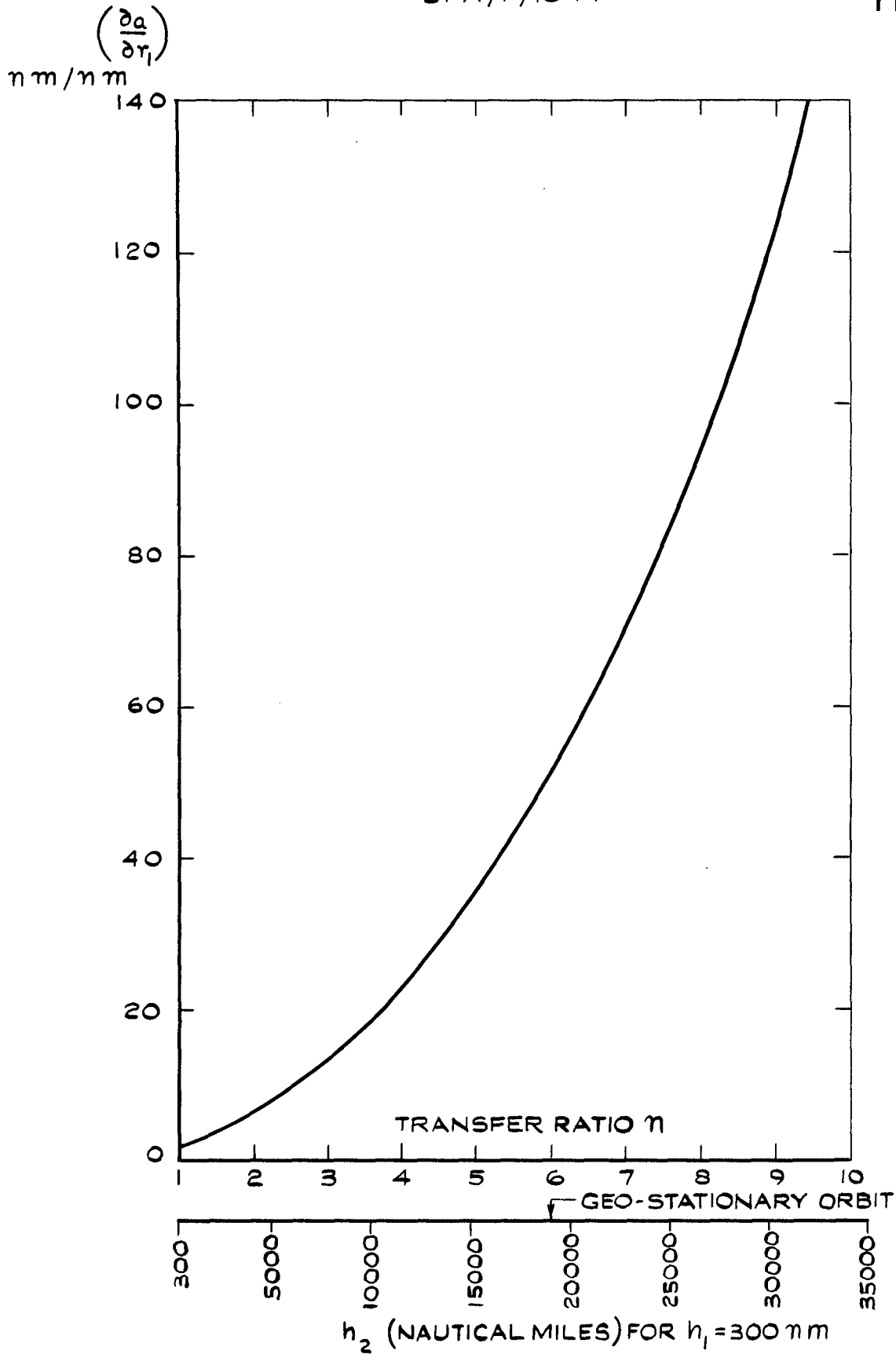

FIG.19 MEAN RADIUS ERROR OF FINAL ORBIT, DUE TO RADIAL POSITION ERROR δr_1 AT START OF TRANSFER

Fig.20

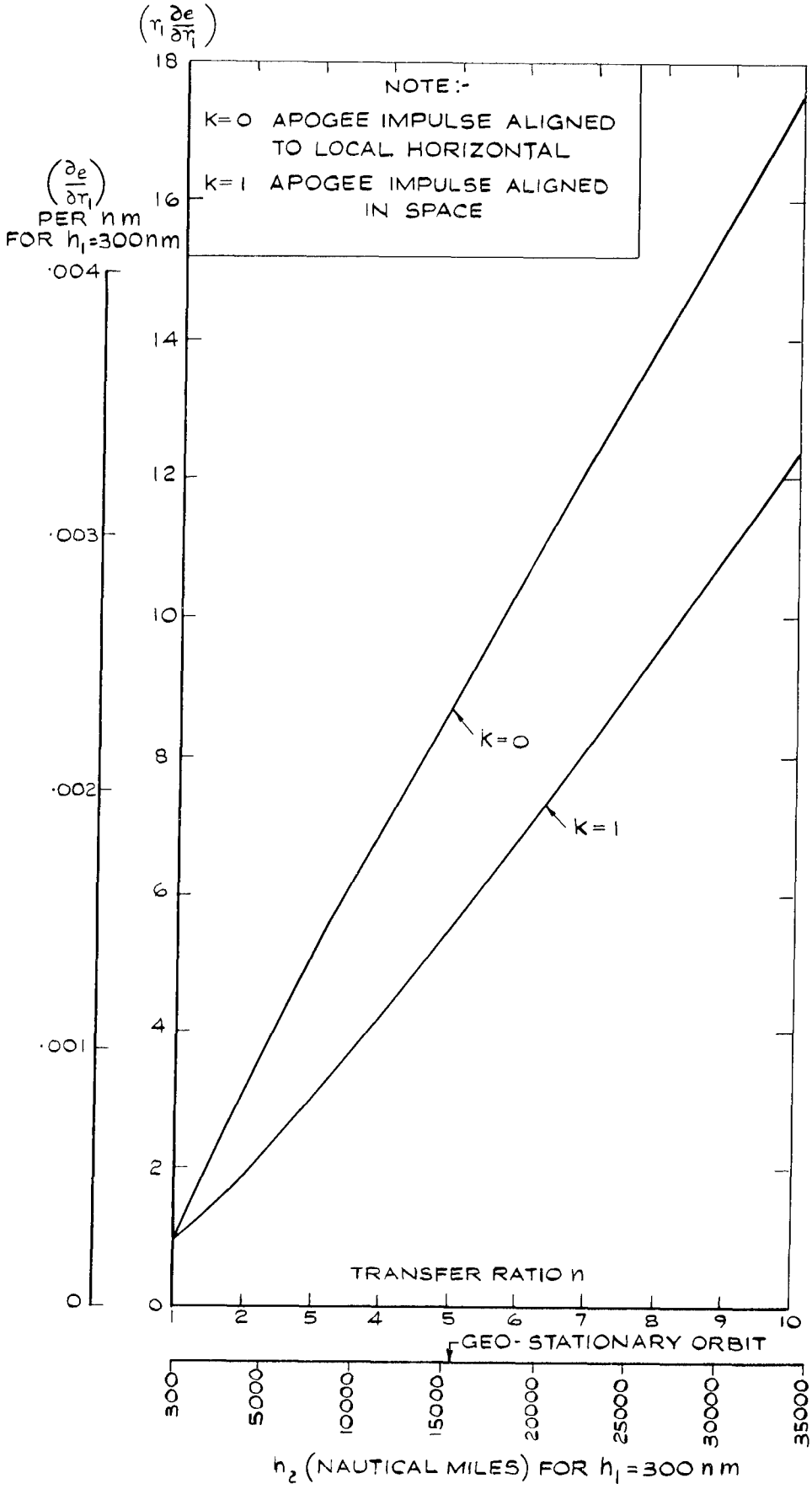

FIG.20 ECCENTRICITY OF FINAL ORBIT, DUE TO RADIAL POSITION ERROR δr_1 AT START OF TRANSFER

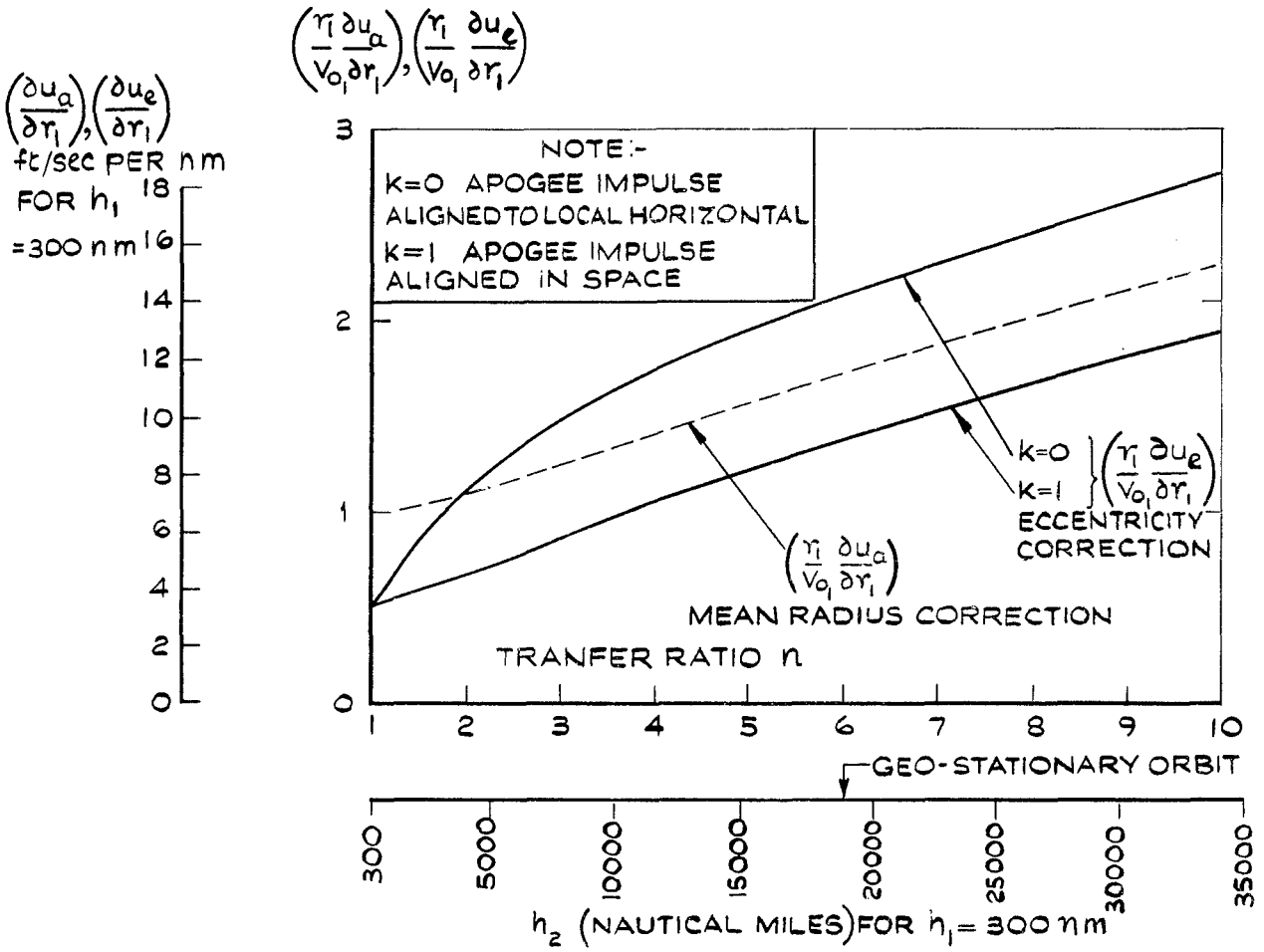

FIG.21 VELOCITIES REQUIRED TO CORRECT MEAN RADIUS AND ECCENTRICITY ERRORS OF FINAL ORBIT, DUE TO RADIAL POSITION ERROR δr_1 AT START OF TRANSFER

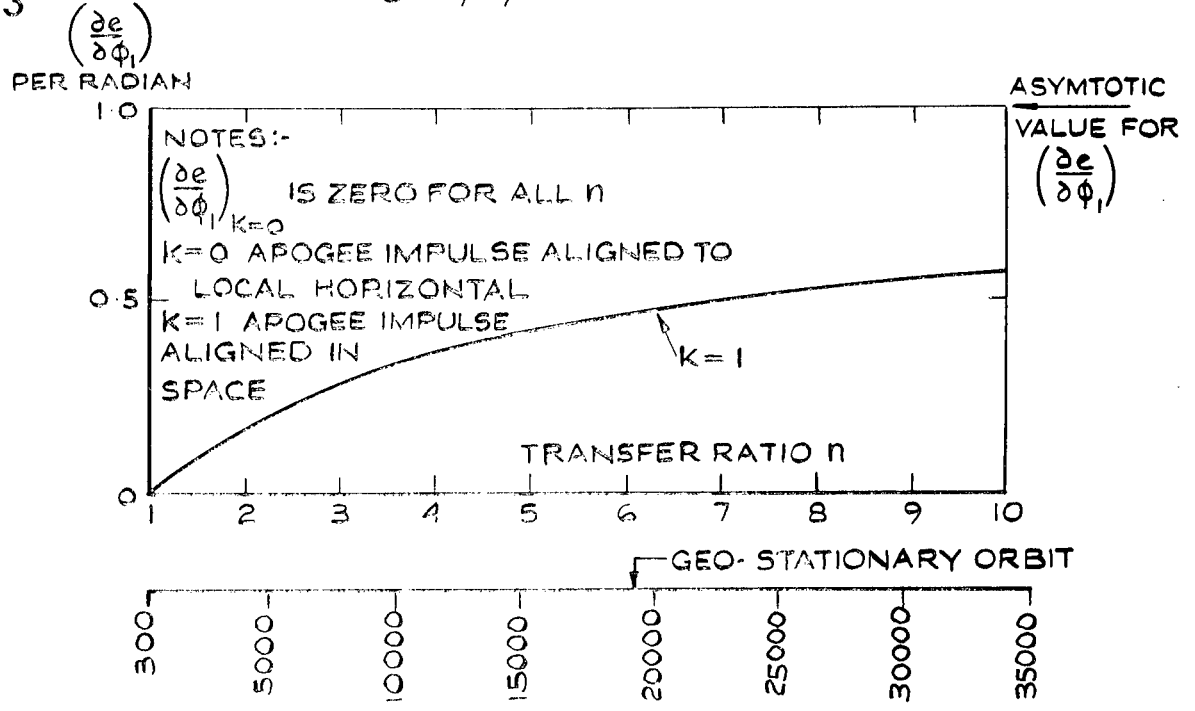

FIG.22 ECCENTRICITY OF FINAL ORBIT, DUE TO ANGULAR RANGE ERROR $\delta\phi_1$ AT START OF TRANSFER

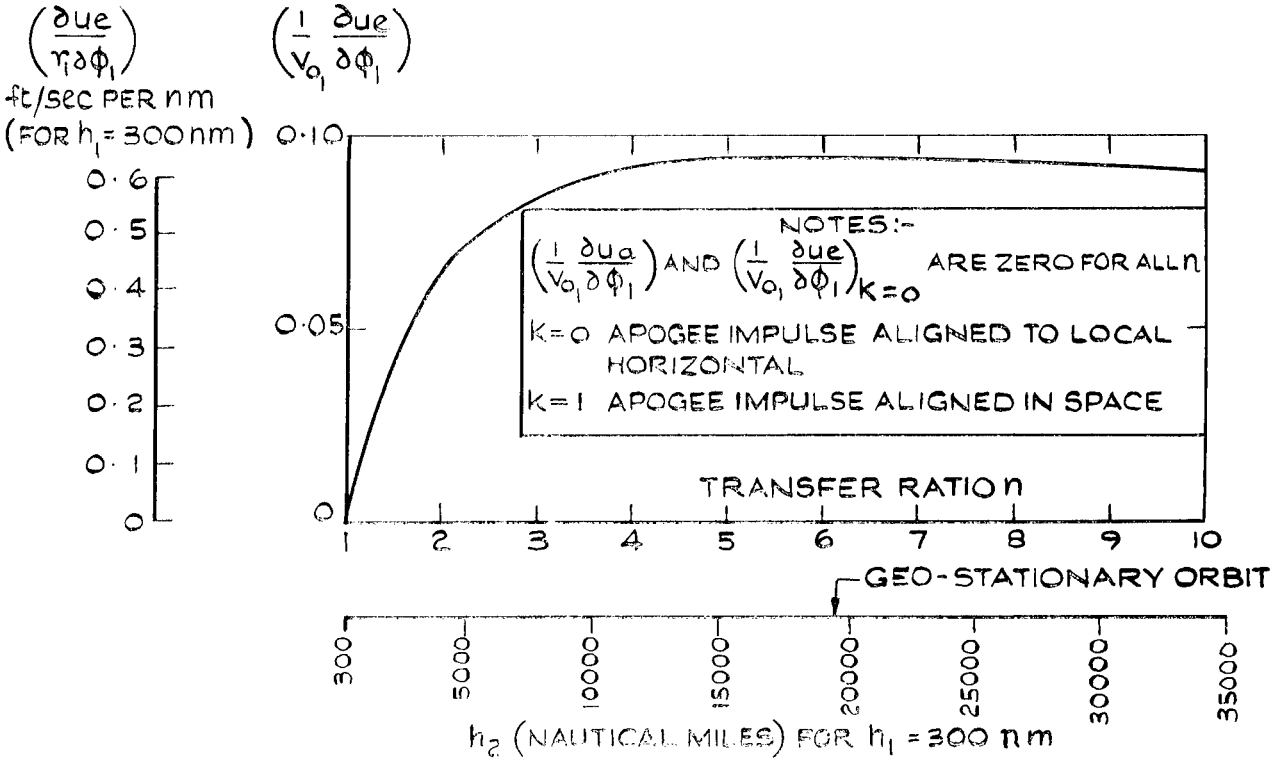

FIG.23 VELOCITY REQUIRED TO CORRECT ECCENTRICITY ERROR OF FINAL ORBIT, DUE TO RANGE ERROR $r_1\delta\phi_1$ AT START OF TRANSFER

Smith, Keith

629.19.077.3 :
629.19.077.2

THE EFFECT OF TRANSFER INJECTION ERRORS UPON THE ACCURACY OF HIGH CIRCULAR ORBITS

Royal Aircraft Establishment Technical Report No.65153 July 1965

First-order relationships between the position and velocity errors at start and end of a Hohmann transfer are derived in a two-dimensional analysis. The results are then used to evaluate the effects of uncorrected first injection errors upon the mean radius and eccentricity of the final (nominally circular) orbit, assuming perfect application of the final impulsive velocity.

Finally the mean radius and eccentricity errors are expressed in terms of post-orbital velocities required for nulling, such as would be required in station-keeping communication satellite systems.

Smith, Keith

629.19.077.3 :
629.19.077.2

THE EFFECT OF TRANSFER INJECTION ERRORS UPON THE ACCURACY OF HIGH CIRCULAR ORBITS

Royal Aircraft Establishment Technical Report No.65153 July 1965

First-order relationships between the position and velocity errors at start and end of a Hohmann transfer are derived in a two-dimensional analysis. The results are then used to evaluate the effects of uncorrected first injection errors upon the mean radius and eccentricity of the final (nominally circular) orbit, assuming perfect application of the final impulsive velocity.

Finally the mean radius and eccentricity errors are expressed in terms of post-orbital velocities required for nulling, such as would be required in station-keeping communication satellite systems.

Smith, Keith

629.19.077.3 :
629.19.077.2

THE EFFECT OF TRANSFER INJECTION ERRORS UPON THE ACCURACY OF HIGH CIRCULAR ORBITS

Royal Aircraft Establishment Technical Report No.65153 July 1965

First-order relationships between the position and velocity errors at start and end of a Hohmann transfer are derived in a two-dimensional analysis. The results are then used to evaluate the effects of uncorrected first injection errors upon the mean radius and eccentricity of the final (nominally circular) orbit, assuming perfect application of the final impulsive velocity.

Finally the mean radius and eccentricity errors are expressed in terms of post-orbital velocities required for nulling, such as would be required in station-keeping communication satellite systems.

Smith, Keith

629.19.077.3 :
629.19.077.2

THE EFFECT OF TRANSFER INJECTION ERRORS UPON THE ACCURACY OF HIGH CIRCULAR ORBITS

Royal Aircraft Establishment Technical Report No.65153 July 1965

First-order relationships between the position and velocity errors at start and end of a Hohmann transfer are derived in a two-dimensional analysis. The results are then used to evaluate the effects of uncorrected first injection errors upon the mean radius and eccentricity of the final (nominally circular) orbit, assuming perfect application of the final impulsive velocity.

Finally the mean radius and eccentricity errors are expressed in terms of post-orbital velocities required for nulling, such as would be required in station-keeping communication satellite systems.

DETACHABLE ABSTRACT CARDS